Elettra
Sincrotrone
Trieste

Joint ICTP-IAEA Workshop on Advances in X-ray Instrumentation for Cultural Heritage Applications

13 - 17 July 2015

ICTP, Trieste (Italy)

Introduction to x-ray absorption spectroscopy

Giuliana Aquilanti
Elettra – Sincrotrone Trieste

giuliana.aquilanti@elettra.eu

Outline

- X-ray absorption
- X-ray absorption fine structure
- XANES
- Some examples of EXAFS and XANES studies for cultural heritage

Outline

- X-ray absorption
- X-ray absorption fine structure
- XANES
- Some examples of EXAFS and XANES studies for cultural heritage

giuliana.aquilanti@elettra.eu

Spectroscopic methods

- They measure the response of a system as a function of energy
- The energy that is scanned can be that of the incident beam or the energy of the outgoing particles (photons in x-ray fluorescence, electrons in photoelectron spectroscopy)
- In all cases, the incident radiation is synchrotron light, which is absorbed, resulting in an ejection of an electron (photoelectric effect)

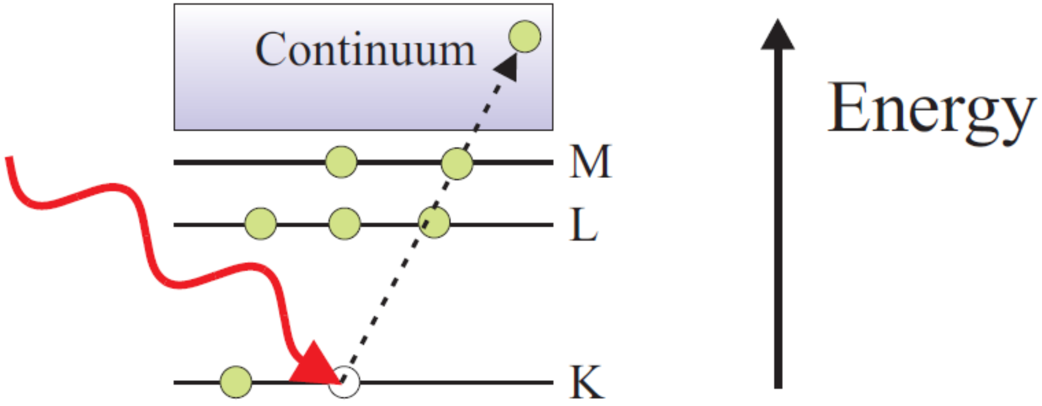

Photoelectric absorption

An x-ray is absorbed by an atom, and the excess energy is transferred to an electron, which is expelled from the atom, leaving it ionized.

giuliana.aquilanti@elettra.eu

The absorption coefficient - 1

- Quantitatively, the absorption is given by the linear absorption coefficient μ
- μdz : attenuation of the beam through an infinitesimal thickness dz at a depth z from the surface

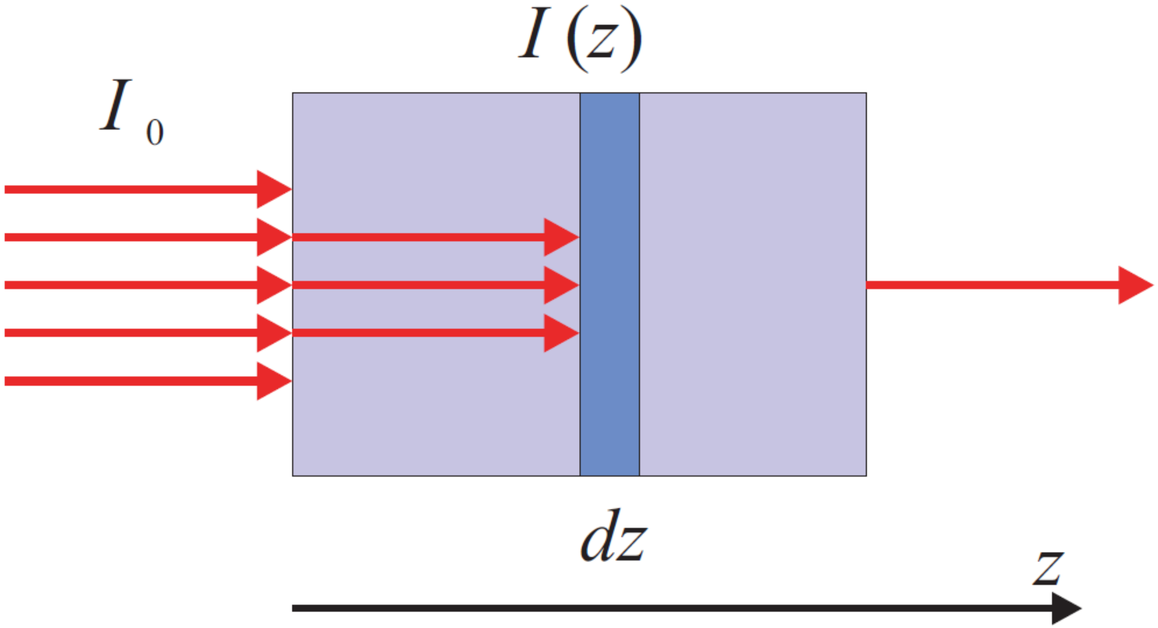

giuliana.aquilanti@elettra.eu

The absorption coefficient - 2

The intensity $I(z)$ through the sample fulfills the condition

$$-dI = I(z)\mu dz$$

which leads to the differential equation

$$dI/I(z) = -\mu dz$$

If $I(z=0) = I_0$, (I_0 : incident beam intensity at $z=0$) then

$$I(z) = I_0 e^{-\mu z}$$

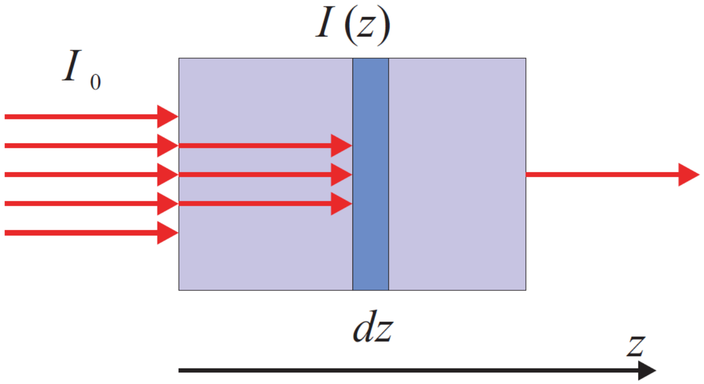

The absorption coefficient - 3

$$I(z) = I_0 e^{-\mu z} \Rightarrow \ln I_0 / I = \mu z$$

Experimentally, μ can be determined as the ratio of the beam intensities with and without the samples (or beam intensity before and after the sample)

giuliana.aquilanti@elettra.eu

Absorption measurements in real life

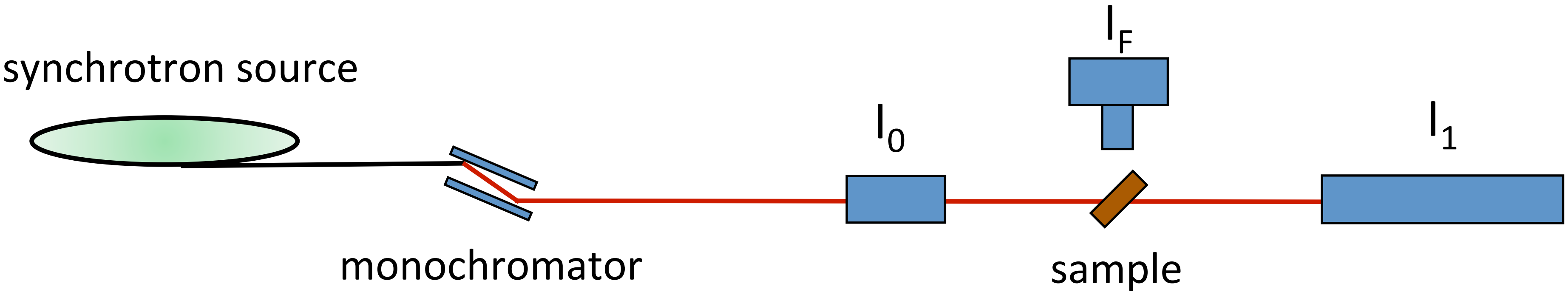

Transmission

The absorption is measured directly by measuring what is transmitted through the sample

Fluorescence

The re-filling the deep core hole is detected. Typically the fluorescent X-ray is measured

giuliana.aquilanti@elettra.eu

XAFS at Elettra

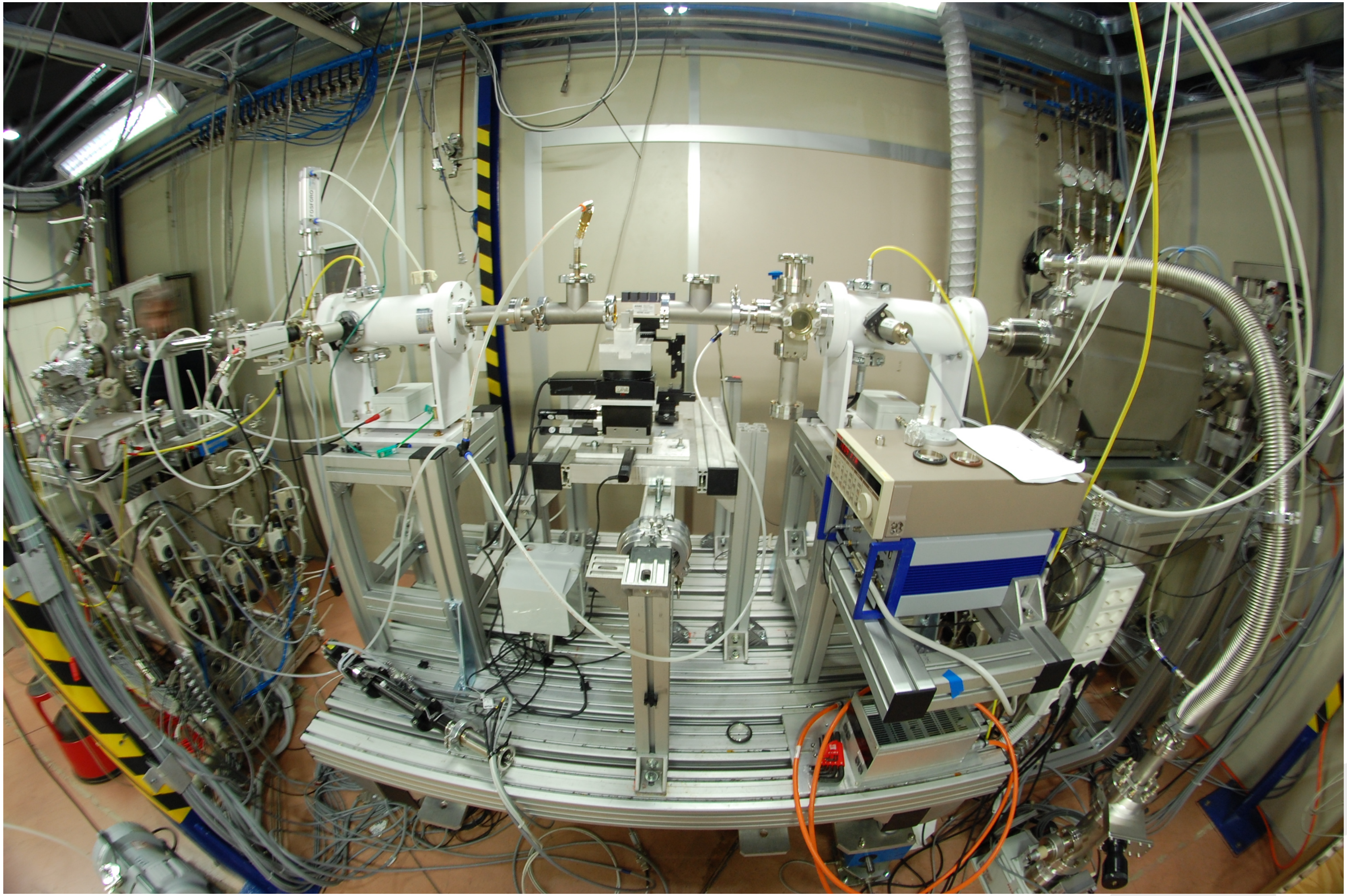

giuliana.aquilanti@elettra.eu

Atomic cross section

$$\mu = \rho_{at}\boldsymbol{\sigma_a} = (\rho_m N_A/A)\boldsymbol{\sigma_a}$$

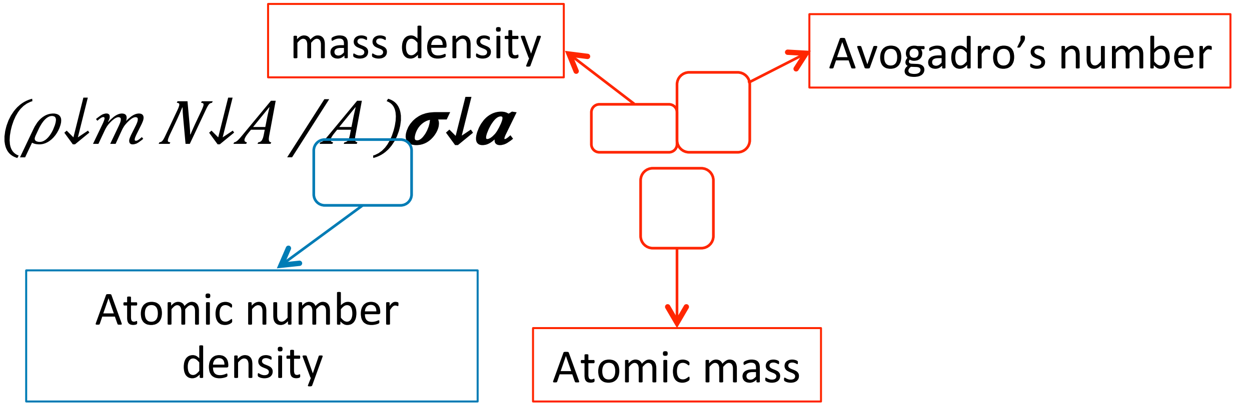

mass density

Avogadro’s number

Atomic number density

Atomic mass

$$\sigma_a\,[\mathrm{cm}^2]$$

$$\sigma_a\,[barn] \qquad 1\ barn = 10^{-28}\ \mathrm{m}^2$$

$$\sigma_a\,[\mathrm{cm}^2/\mathrm{g}] = N_A/A\ \sigma_a\,[\mathrm{cm}^2] = \mu/\rho_m$$

giuliana.aquilanti@elettra.eu

μ vs E and μ vs Z

μ depends strongly on:

- x-ray energy E
- atomic number Z
- density ρ
- atomic mass A

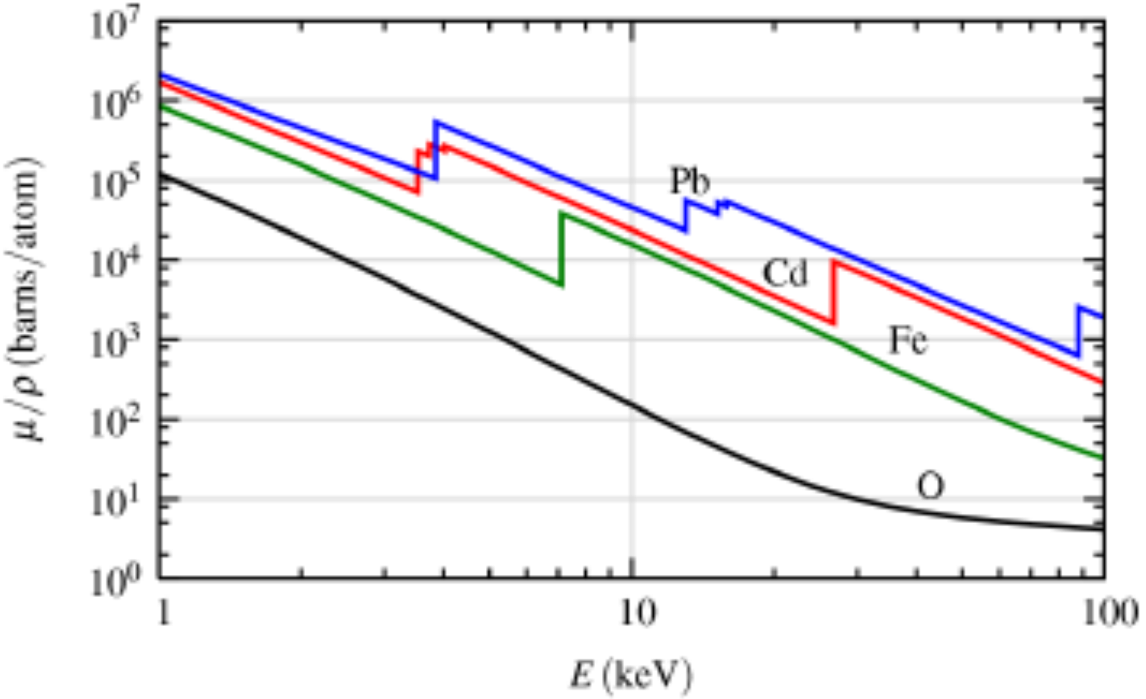

In addition, μ has sharp *absorption edges* corresponding to the characteristic core-level energy of the atom which originate when the photon energy becomes high enough to extract an electron from a deeper level

giuliana.aquilanti@elettra.eu

Absorption edges and nomenclature

Table 2.1 *Correspondence between x-ray absorption edges and their electronic configurations.*

Edge	Configuration	Edge	Configuration
K	$1s$	N_1	$4s$
L_1	$2s$	N_2	$4p_{1/2}$
L_2	$2p_{1/2}$	N_3	$4p_{3/2}$
L_3	$2p_{3/2}$	N_4	$4d_{3/2}$
M_1	$3s$	N_5	$4d_{5/2}$
M_2	$3p_{1/2}$	N_6	$4f_{5/2}$
M_3	$3p_{3/2}$	N_7	$4f_{7/2}$
M_4	$3d_{3/2}$	O_1	$5s$
M_5	$3d_{5/2}$	O_2	$5p_{1/2}$

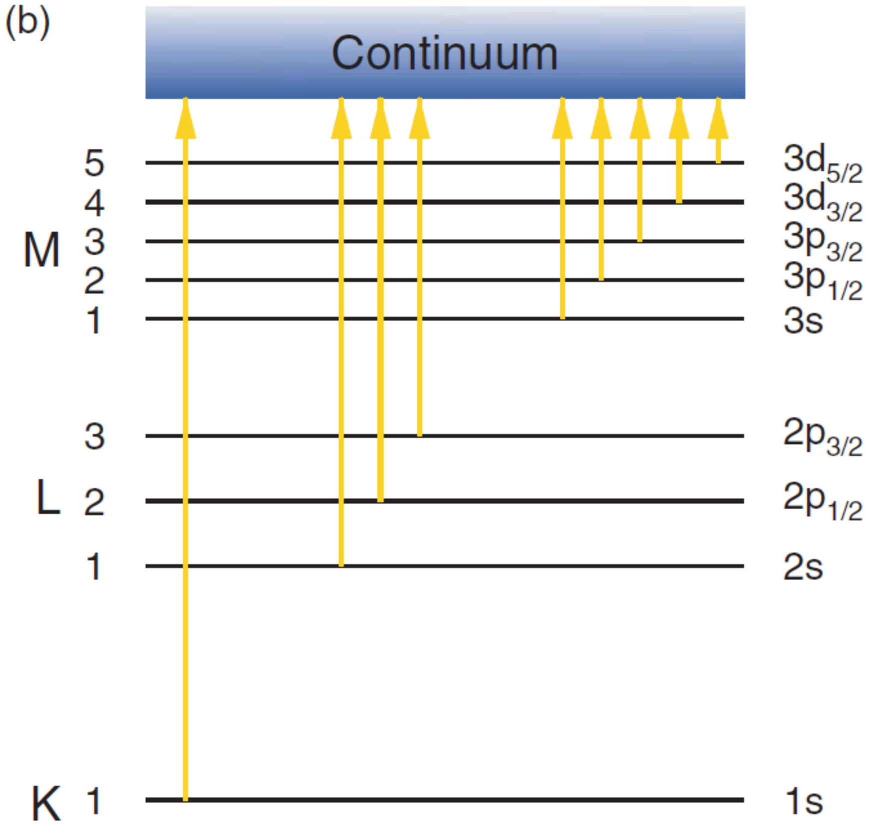

Absorption edge energies

The energies of the *K* absorption edges go roughly as $E_K \sim Z^2$

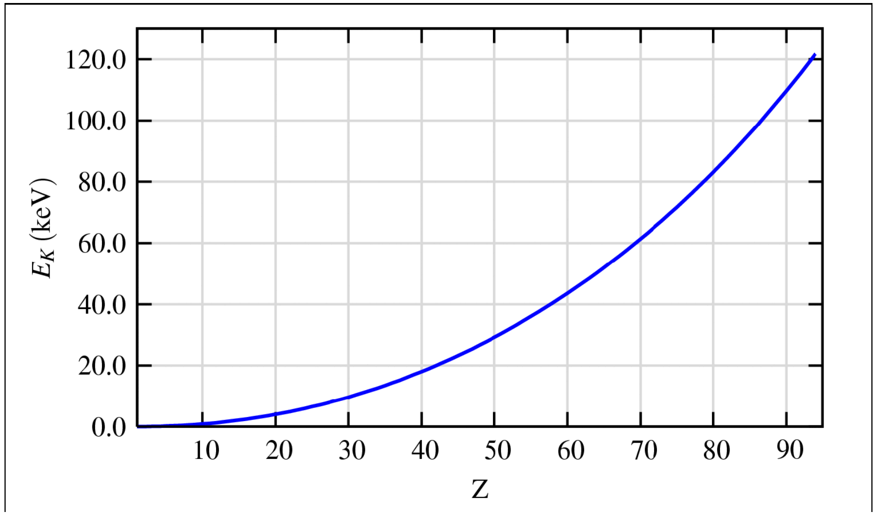

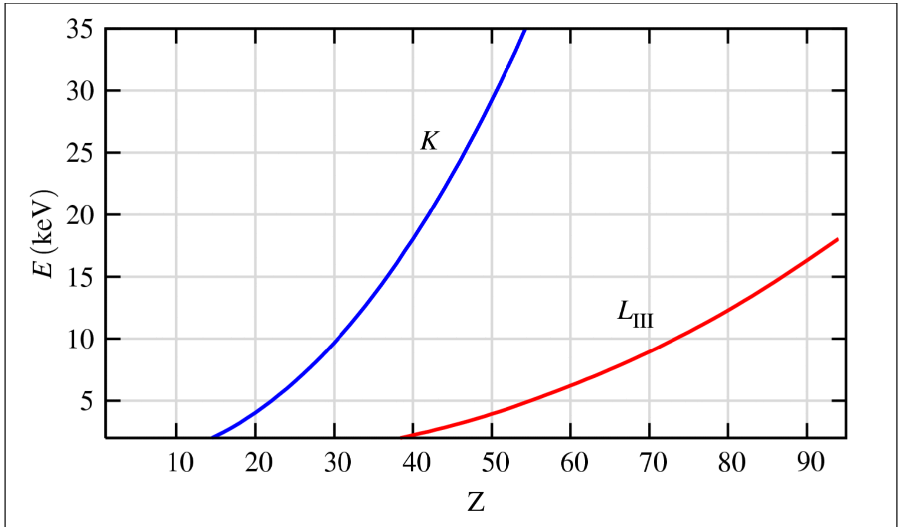

All elements with Z > 16 have either a *K*-, or *L*- edge between 2 and 35 keV, which can be accessed at many synchrotron sources

giuliana.aquilanti@elettra.eu

De-excitation process

Absorption → Excited state → Decay to the ground state

Core hole +
photoelectron

X-ray Fluorescence

An x-ray with energy equal to the difference of the core-levels is emitted

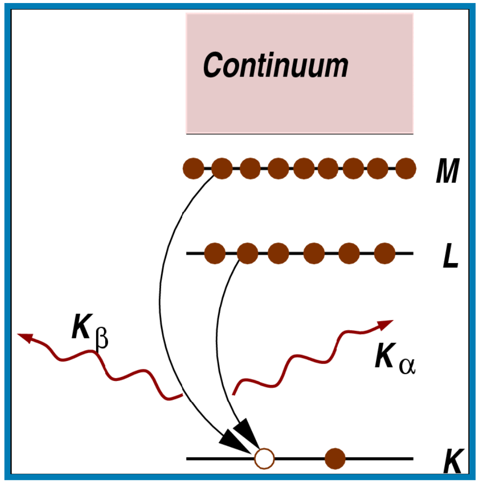

Auger Effect

An electron is promoted to the continuum from another core-level

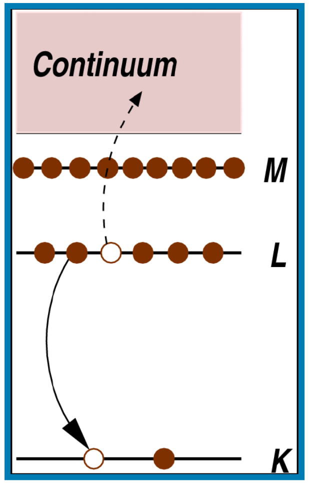

X-ray fluorescence and Auger emission occur at discrete energies characteristic of the absorbing atom, and can be used to identify the absorbing atom

Core-hole lifetime ($\tau_h \sim 10^{-15} - 10^{-16}$ s)

Total de-excitation probability per unit time

The deeper the core hole and the larger the atomic number Z

⬇

The larger the number of upper levels from which
an electron can drop to fill the hole

⬇

The shorter the core hole lifetime

τ_h is un upper limit to the time allowed to the photoelectron for probing the local structure surrounding the absorbing atom

From the time-energy uncertainty relation: $\Gamma_h \simeq \hbar/\tau_h$ the core hole lifetime is associated to the energy width of the excited state Γ_h *(core hole broadening)* which contributes to the resolution of the x-ray absorption experimental spectra

giuliana.aquilanti@elettra.eu

K-edge core hole broadening

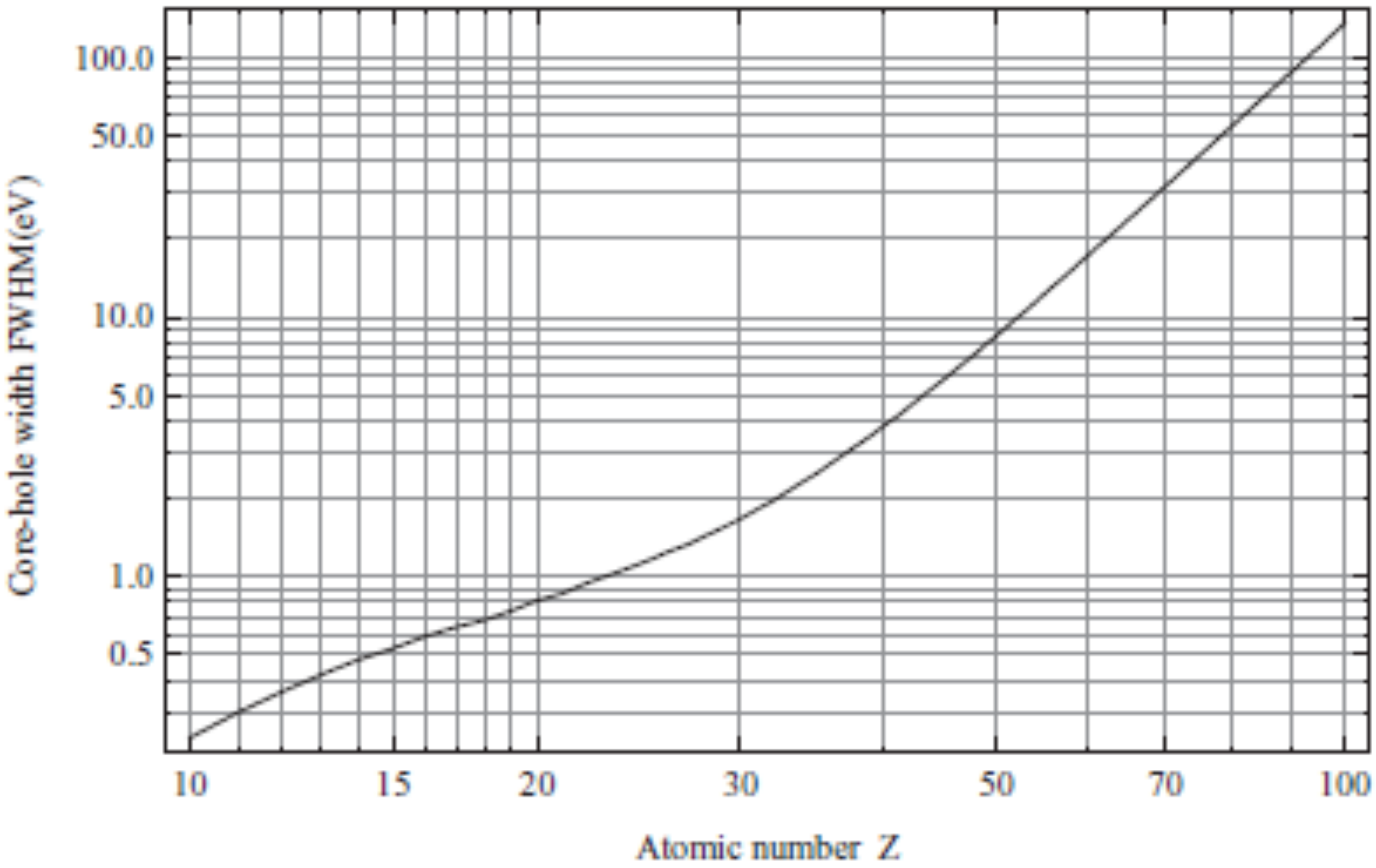

Outline

- X-ray absorption
- X-ray absorption fine structure
- XANES
- Some examples of EXAFS and XANES studies for cultural heritage

giuliana.aquilanti@elettra.eu

X-ray Absorption Fine Structure

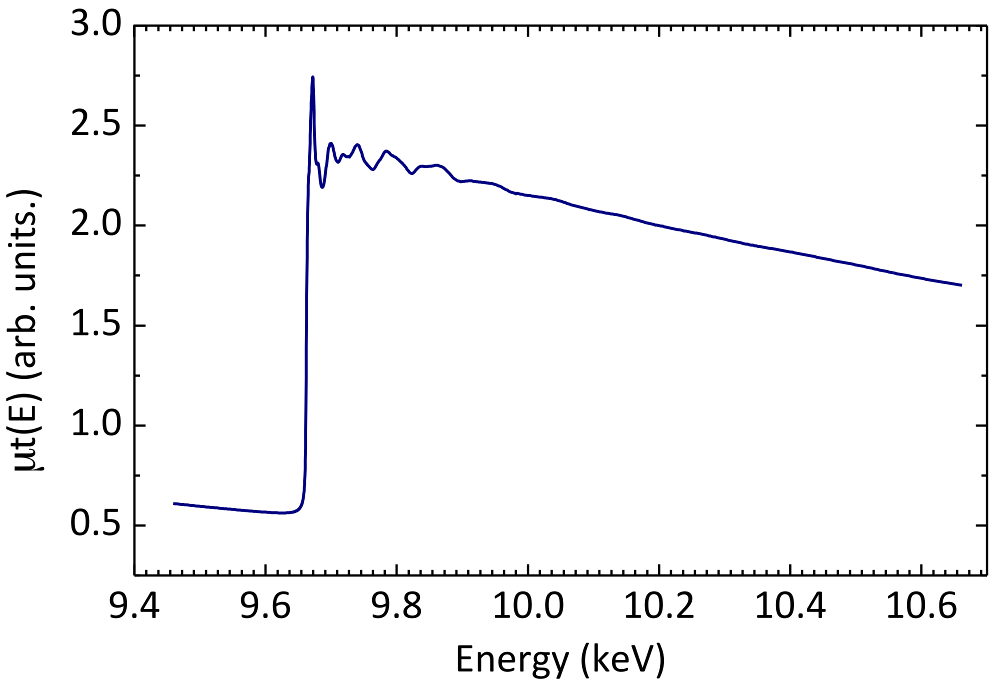

What? Oscillatory behaviour of the of the x-ray absorption as a function of photon energy beyond an absorption edge

When? Non isolated atoms

Why? Proximity of neighboring atoms strongly modulates the absorption coefficient

A little history

1895	Discovery of x-rays (Röngten) (high penetration depth)
1912	First x-ray diffraction experiments (Laue, Bragg)
1913	Bohr's atom electron energy levels
1920	First experimental observation of fine structure
1931	First attempt to explain XAFS in condensed matter (Krönig)
.	
.	
1970	Availability of synchrotron radiation sources for XAFS
1971	XAFS becomes a quantitative tool for structure determination

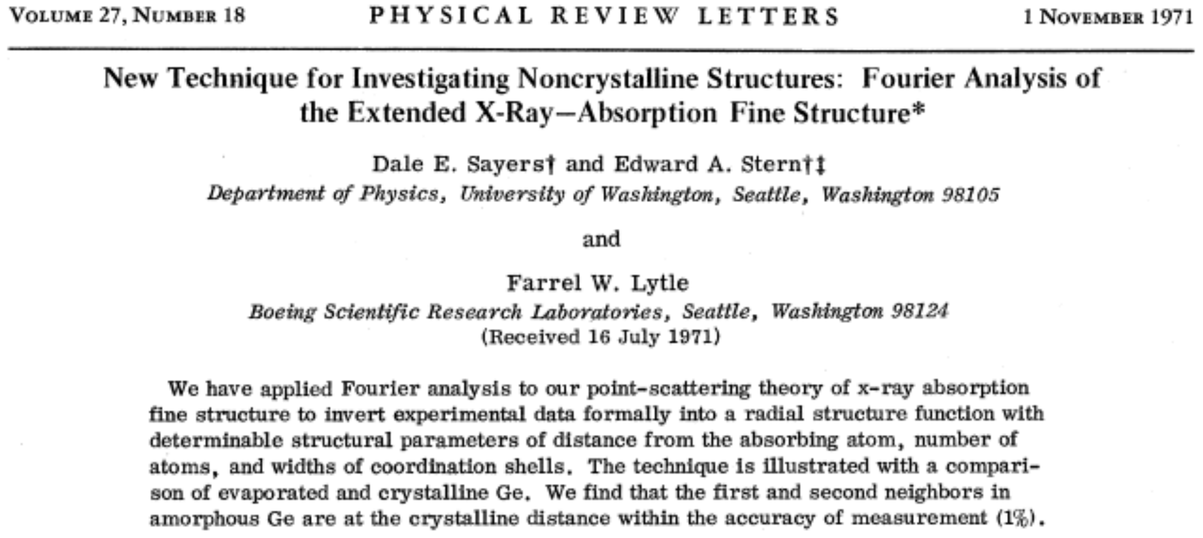

Volume 27, Number 18 PHYSICAL REVIEW LETTERS 1 November 1971

New Technique for Investigating Noncrystalline Structures: Fourier Analysis of the Extended X-Ray—Absorption Fine Structure*

Dale E. Sayers† and Edward A. Stern†‡
Department of Physics, University of Washington, Seattle, Washington 98105

and

Farrel W. Lytle
Boeing Scientific Research Laboratories, Seattle, Washington 98124
(Received 16 July 1971)

We have applied Fourier analysis to our point-scattering theory of x-ray absorption fine structure to invert experimental data formally into a radial structure function with determinable structural parameters of distance from the absorbing atom, number of atoms, and widths of coordination shells. The technique is illustrated with a comparison of evaporated and crystalline Ge. We find that the first and second neighbors in amorphous Ge are at the crystalline distance within the accuracy of measurement (1%).

XANES and EXAFS - 1

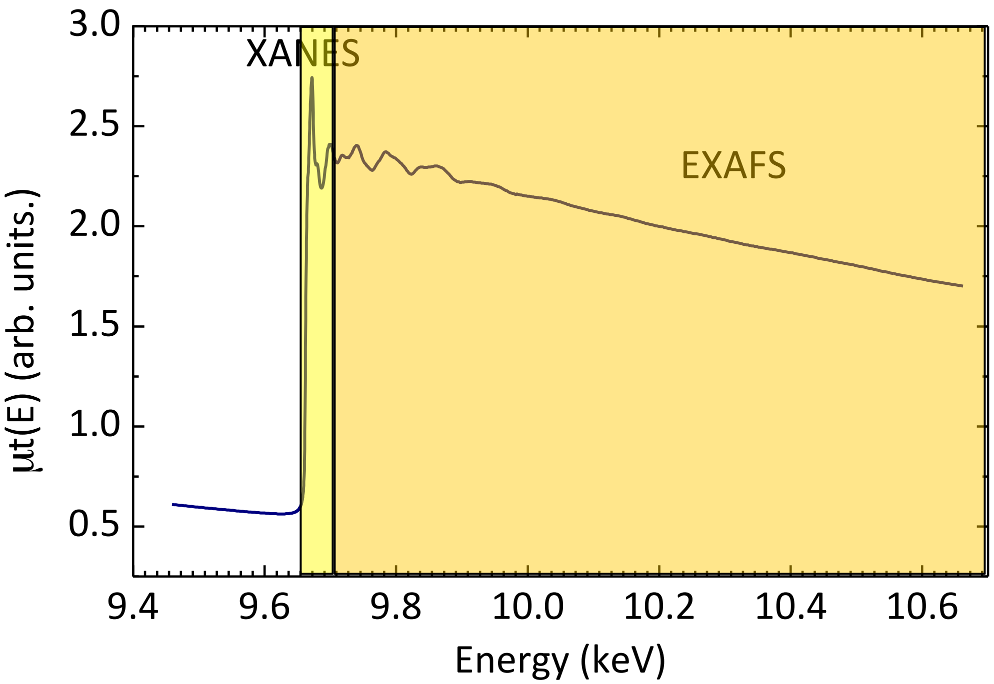

X-ray
Absorption
Near
Edge
Structure

up to ~ 60 eV
above the edge

Extended
X-ray
Absorption
Fine
Structure

from ~ 60 eV
to 1200 eV
above the edge

giuliana.aquilanti@elettra.eu

XANES and EXAFS - 2

XANES ⟸ same physical origin ⟹ EXAFS

transitions to
unfilled bound states,
nearly bound states,
continuum

⇓

- Oxidation state
- Coordination chemistry (tetrahedral, octahedral) of the absorbing atom
- Orbital occupancy

transitions to
the continuum

⇓

- Radial distribution of atoms around the photoabsorber (bond distance, number and type of neighbours)

EXAFS qualitatively – isolated atom

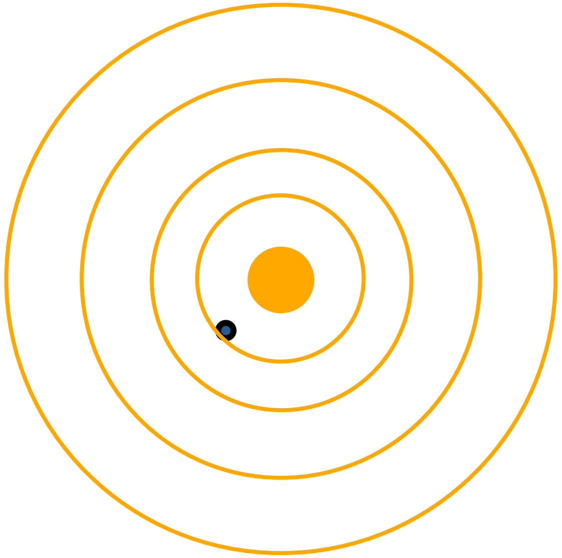

- X-ray photon with enough energy ejects one core (photo)electron (photoelectric effect)

$$E_k = E_{h\nu} - E_0 = \frac{p^2}{2m} = \frac{(\hbar k)^2}{2m}$$ Kinetic energy of the p.e.

$$k = \sqrt{[2m(E_{h\nu} - E_0)/\hbar^2]}$$ wavevector of the p.e.

$$\lambda = 2\pi/k$$ wavelength of the p.e.

- The photoelectron can be described by a wave function approximated by a spherical wave

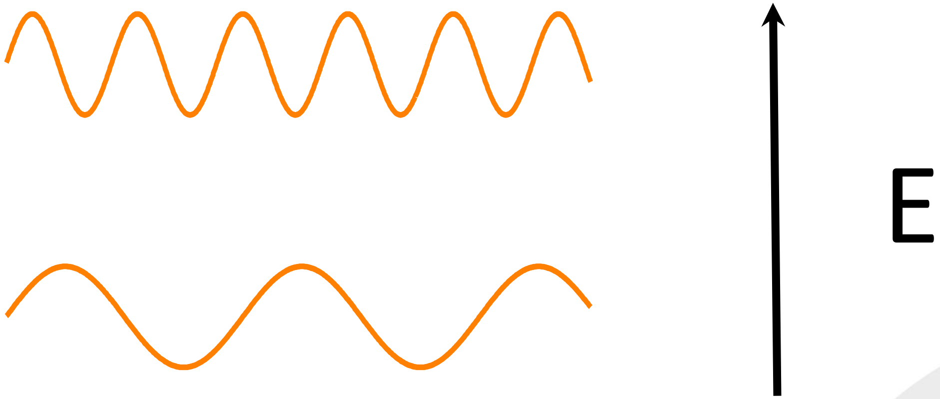

giuliana.aquilanti@elettra.eu

Elettra
Sincrotrone
Trieste

EXAFS qualitatively – condensed matter

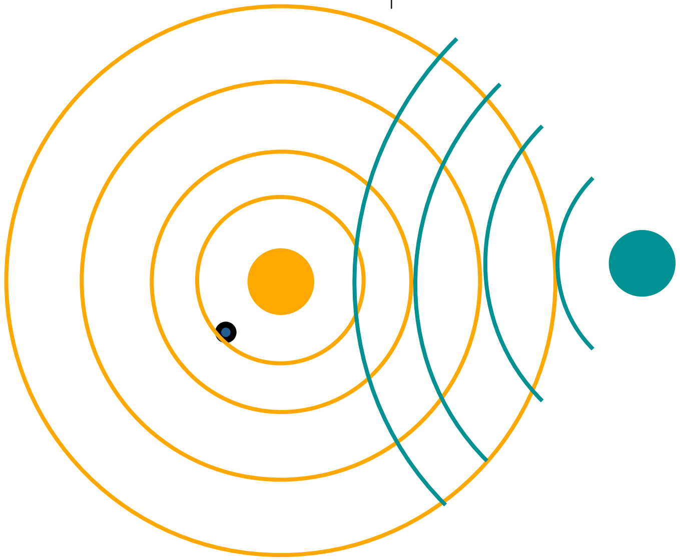

- The photoelectron can scatter from a neighbouring atom giving rise to an incoming spherical wave coming back to the absorbing atom
- The outgoing and ingoing waves may interfere

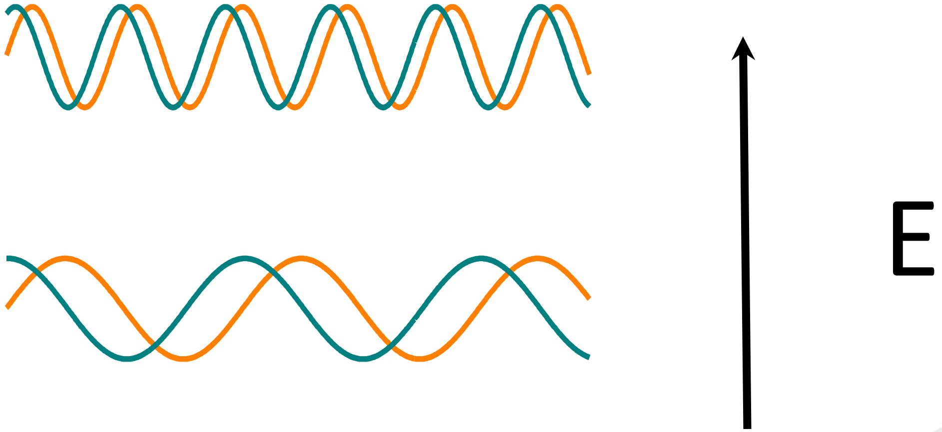

giuliana.aquilanti@elettra.eu

Origin of the fine structure (oscillations)

- The interference between the outgoing and the scattering part of the photoelectron at the absorbing atom changes the probability for an absorption of x-rays i.e. alters the absorption coefficient $\mu(E)$ that is no longer smooth as in isolated atoms, but oscillates.
- In the extreme of destructive interference, when the outgoing and the backscattered waves are completely out of phase, they will cancel each other, which means that no free unoccupied state exists in which the core-electron could be excited to.
- Thus absorption is unlikely to occur and the EXAFS oscillations will have a minimum.
- The phase relationship between outgoing and incoming waves depends on photoelectron wavelength (and so on the energy of x-rays) and interatomic distance R.
- The amplitude is determined by the number and type of neighbours since they determine how strongly the photoelectron will be scattered

giuliana.aquilanti@elettra.eu

Which information

Frequency of the oscillations

⇓

Distance from neighbours

Amplitude of the oscillations

⇓

Number and type of neighbours

Some spectra

Kr gas

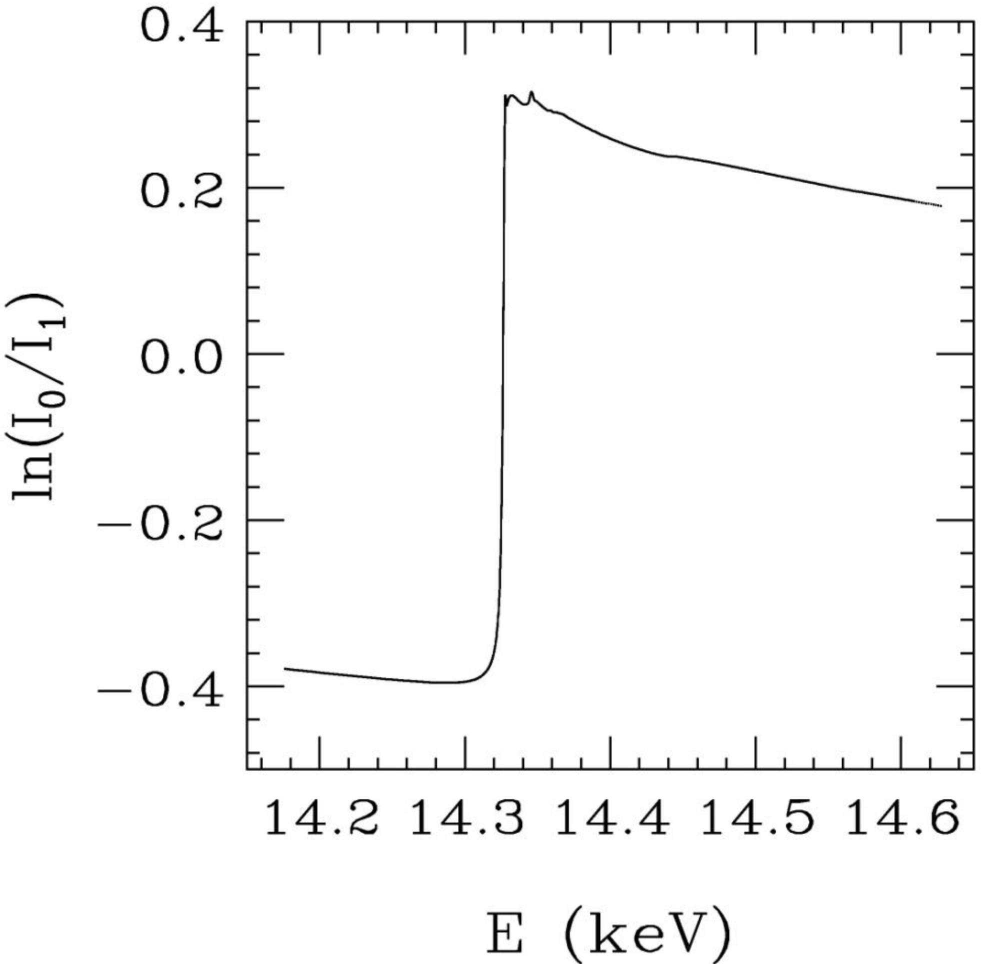

Rh metal

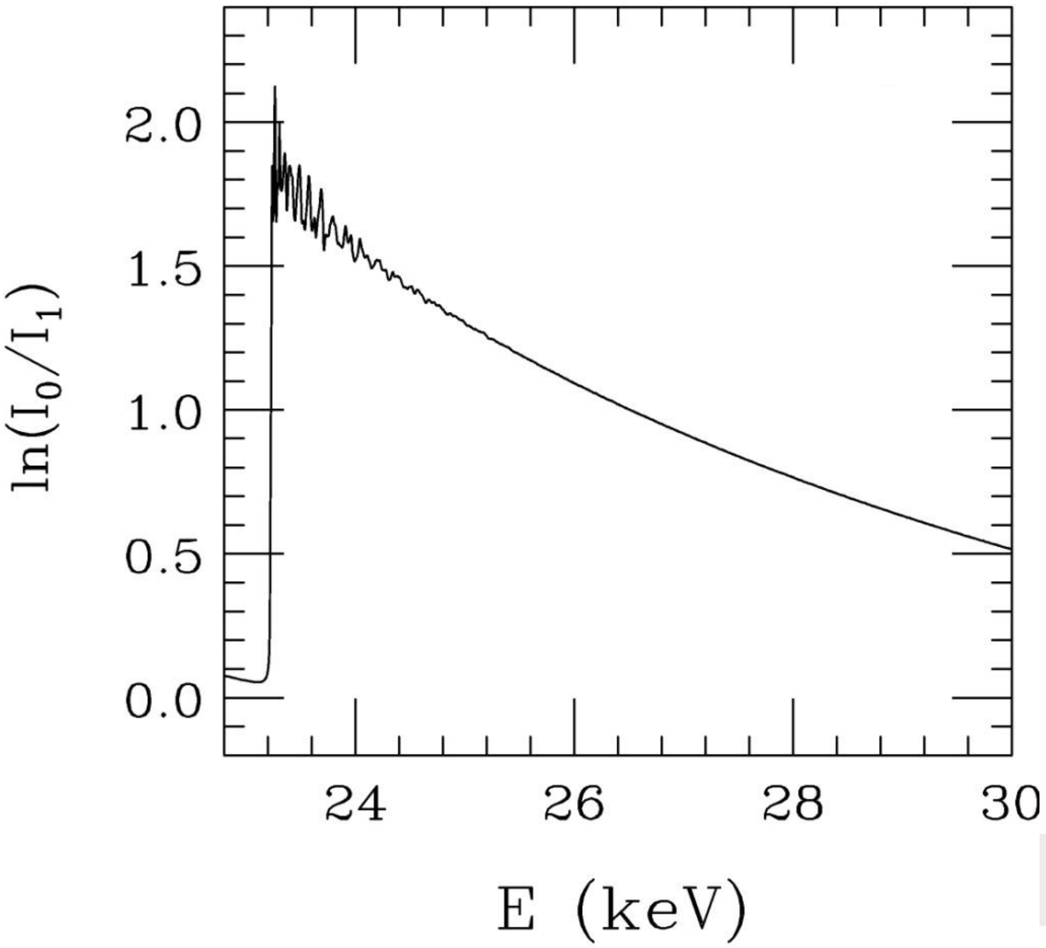

giuliana.aquilanti@elettra.eu

Fermi’s Golden rule

According to the time dependent perturbation theory, the Fermi’s Golden rule gives the transition rate (probability of transition per unit time) per unit volume between an initial and a final eigenstate due to a perturbation

$$w_{fi} = \frac{2\pi}{\hbar} \left| \langle \Psi_f | \mathcal{H}_{int} | \Psi_i \rangle \right|^2 \rho(E_f)$$

$$\mu = -\frac{1}{I}\frac{dI}{dz} = \sum_f \frac{2\pi c}{\omega^2 A_0^2} N \hbar \omega w_{fi}$$

Sum over
all final states

Number of microscopic
absorbing element
per unit volume

Absorption process

$$\mu \propto \sum_f |\langle \psi_f | \boldsymbol{\varepsilon} \cdot \boldsymbol{r} | \psi_i \rangle|^2 \rho(E_f)$$

photon polarization

Electron position

|i› : initial state of energy E_i

- core electron (*e.g.* 1s electron wave function)
- very localized
- NOT altered by the presence of the neighboring atoms

|f› : final state of energy $E_f = E_i + \hbar\omega$

- core hole + photoelectron
- multibody process
- altered by neighbouring atoms

Initial and final states

Wavefunction of the initial state:

$|i>= Y_{l_0,m_0}(\hat{\mathbf{r}})R^0_{l_0}(r)$ Where l_0 angular momentum of the electron

$Y_{l0,m0}$ spherical harmonic functions

(solution of the angular part of the Schrödinger equation)

For the final state a potential must take into account that the electron moves in the condensed matter

Muffin Tin Potential

Spherical regions centered on each atom in which the potential has a spherical symmetry. Wavefunctions described by a radial + angular part

Interstitial region with a constant potential. Wavefunctions described by plane waves

giuliana.aquilanti@elettra.eu

Dipole selection rules

The dipolar selection rules determine the transition from the initial to the final state

$$\boxed{\begin{aligned} \Delta\ell &= \pm 1 \\ \Delta s &= 0 \\ \Delta j &= \pm 1, 0 \\ \Delta m &= 0 \end{aligned}}$$

EDGE	INITIAL STATE	FINAL STATE
K, L_1	s (ℓ=0)	p (ℓ=1)
L_2, L_3	p (ℓ=1)	s (ℓ=0), d (ℓ=2)

Elettra
Sincrotrone
Trieste

The EXAFS signal $\chi(k)$ - 1

- The EXAFS signal is generally espressed as a function of the wavevector of the photoelectron $k=\sqrt{2m(E_{h\nu}-E_0)/\hbar^2}$
- The oscillatory part of the spectrum contains the structural information
- We define the EXAFS function as $\chi(k)=\frac{\mu-\mu_0}{\Delta\mu_0}$

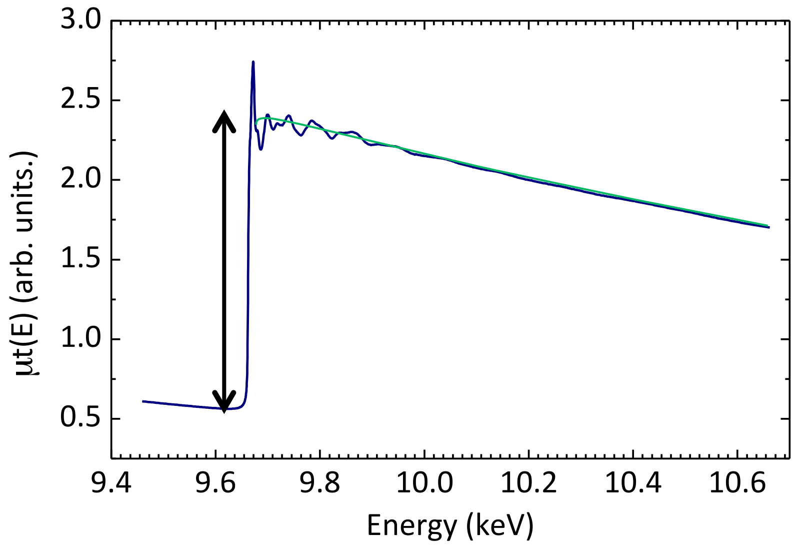

$\mu_0(E)$ Smooth function representing the bare atomic background

$\Delta\mu_0$ Edge step at the absorption edge normalized to one absorption event

giuliana.aquilanti@elettra.eu

The EXAFS signal $\chi(k)$ - 2

XAFS originates from an *interference effect*,
and depends on the wave-nature of the photoelectron.

$\chi(k)$ is often shown weighted by k^2 or k^3 to amplify the oscillations at high-k

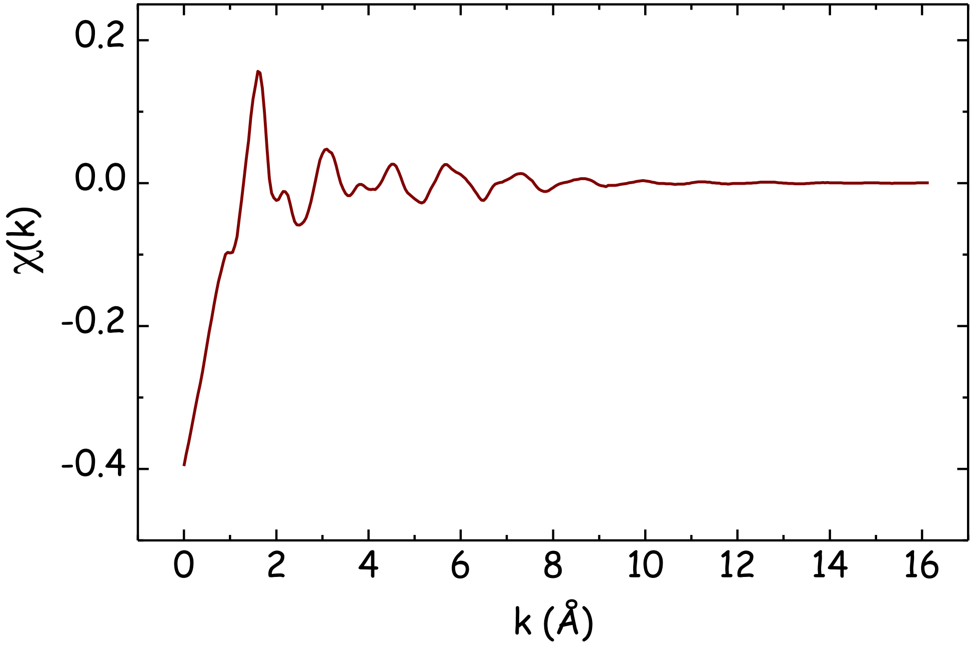

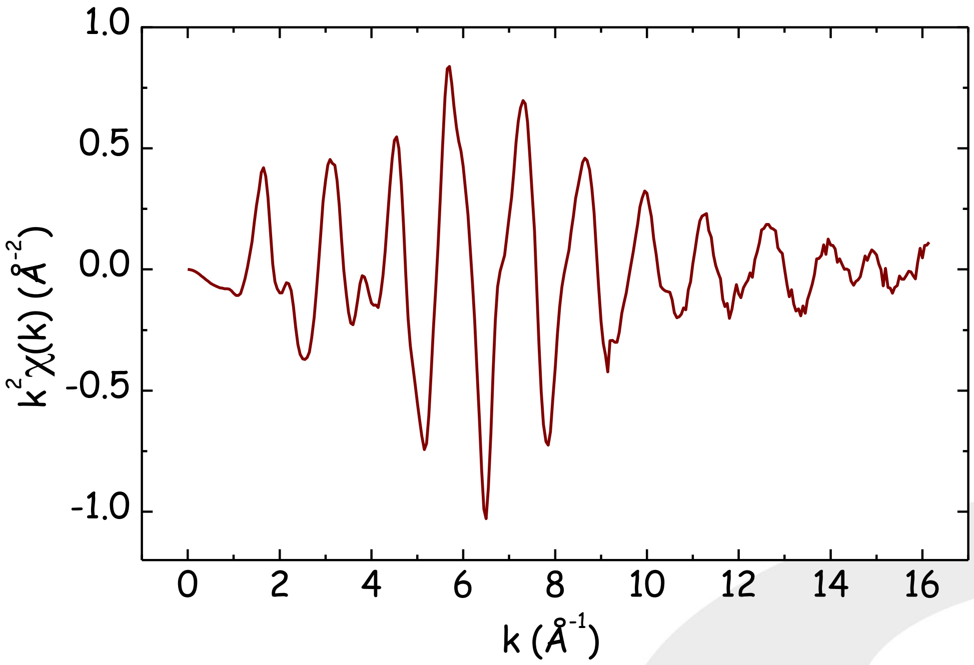

$\chi(k)$: sum of damped waves

χ(k) is the sum of contributions **χ**$_j$(k) from backscattered wavelets:

$$\chi(k) = \sum_j = \chi_j(k)$$

Each **χ**$_j$(k) can be approximated by a *damped* sine wave of the type:

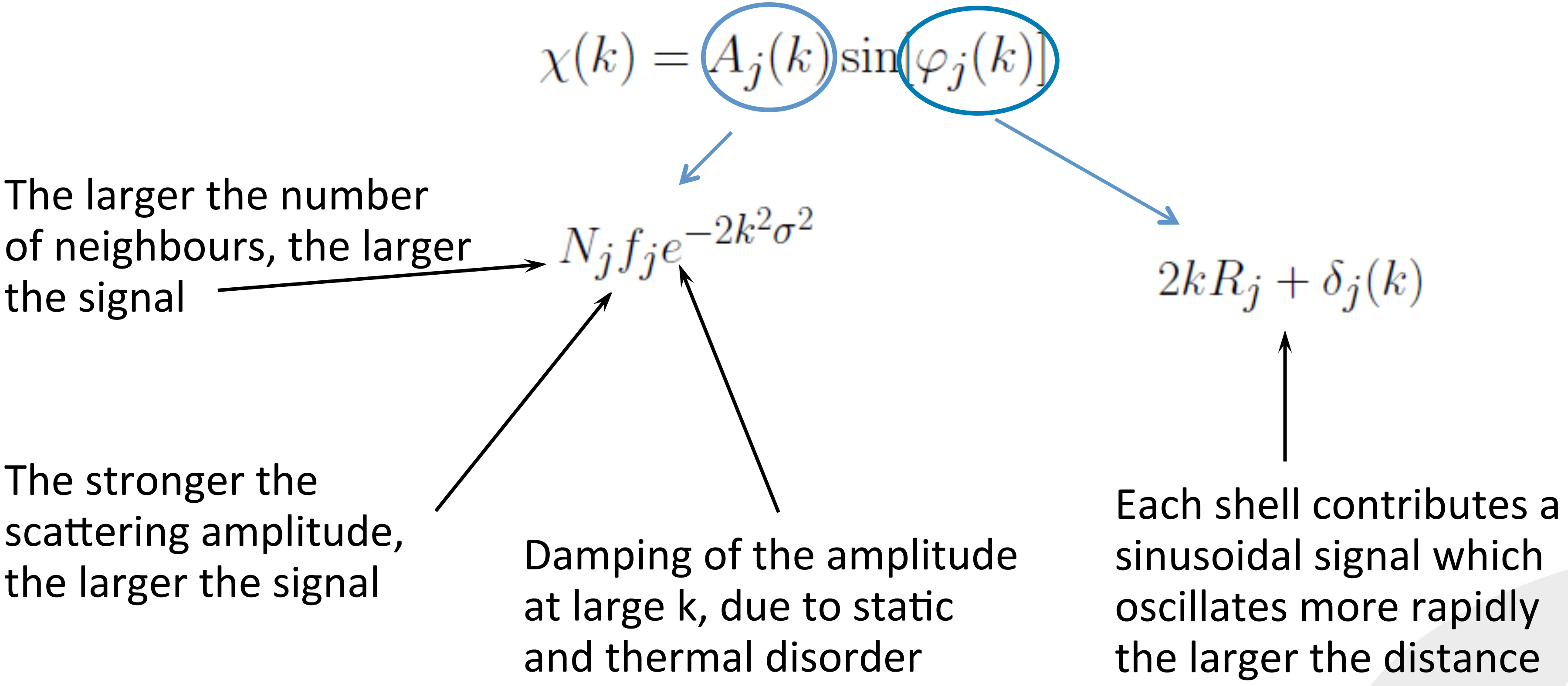

$$\chi(k) = \boxed{A_j(k)} \sin\left[\boxed{\varphi_j(k)}\right]$$

$$N_j f_j e^{-2k^2\sigma^2}$$

$$2kR_j + \delta_j(k)$$

The larger the number of neighbours, the larger the signal

The stronger the scattering amplitude, the larger the signal

Damping of the amplitude at large k, due to static and thermal disorder

Each shell contributes a sinusoidal signal which oscillates more rapidly the larger the distance

EXAFS formula

$$\chi(k) = \sum_j \frac{N_j S_0^2 f_j(k) e^{-2R_j/\lambda(k)}\, e^{-2k^2\sigma_j^2}}{kR_j^{\,2}} \sin[2kR_j + \delta_j(k)]$$

$f(k)$	scattering amplitude	scattering properties of the atoms neighbouring the photoabsorber (depend on the atomic number)
$\delta_j(k)$	phase-shift	

R Distance to the neighbouring atom

N Coordination number of the neighbouring atom

σ^2 Disorder in the neighbouring distance

giuliana.aquilanti@elettra.eu

Amplitudes

The shape of the envelope of each wave is indicative of the nature of backscatterer atom

AgF (rocksalt structure)

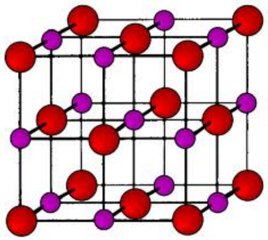

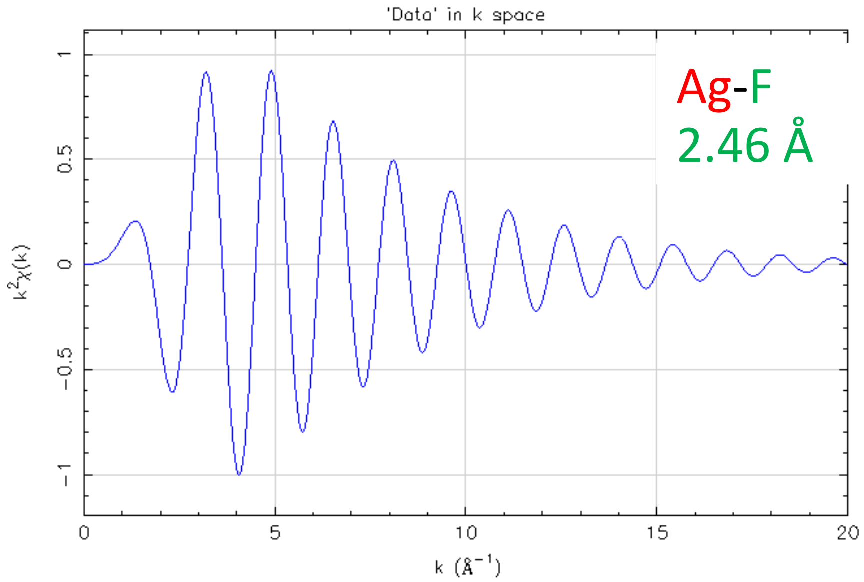

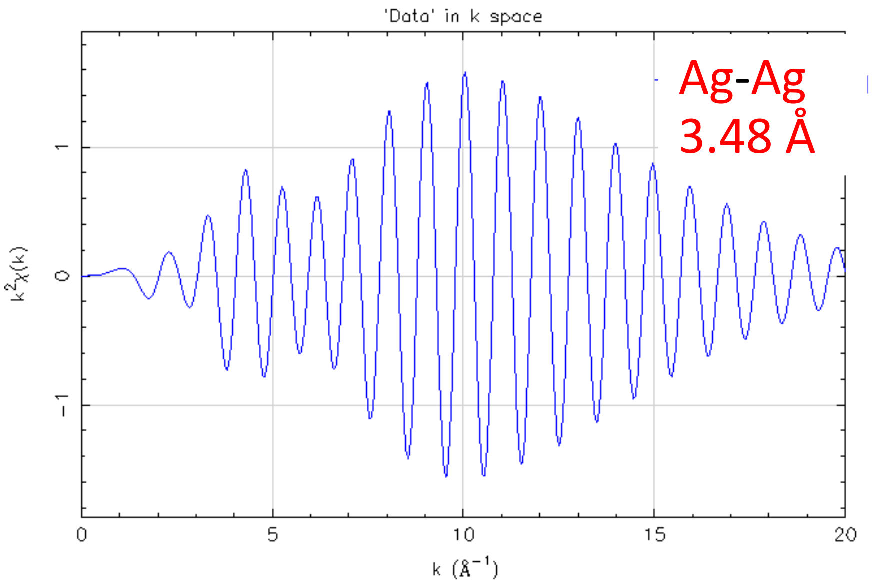

Frequencies

The frequency of the single wave, for the same atomic pair, is indicative of the distance of the backscatterer atom (the lower the frequency the closer the neighbour)

AgF (rocksalt structure)

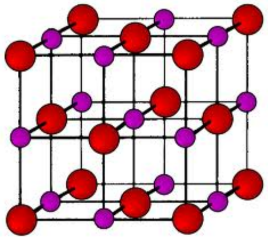

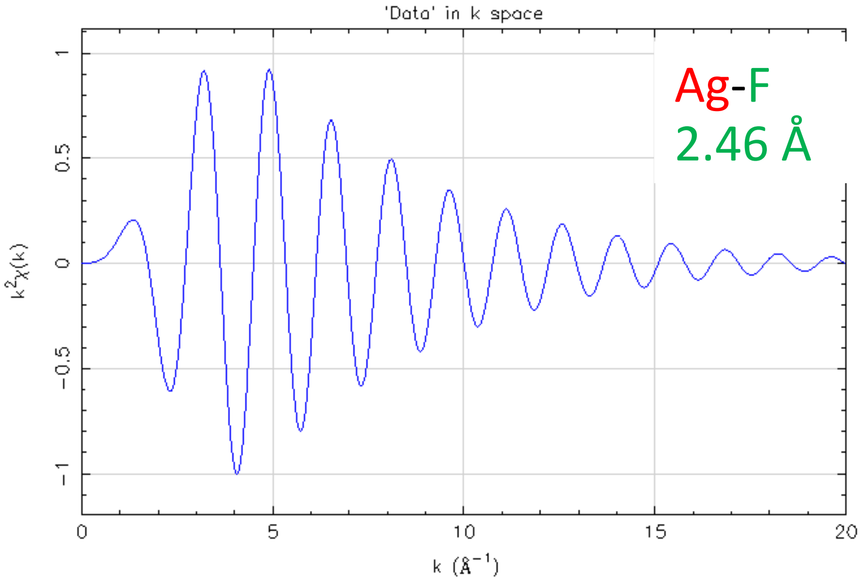

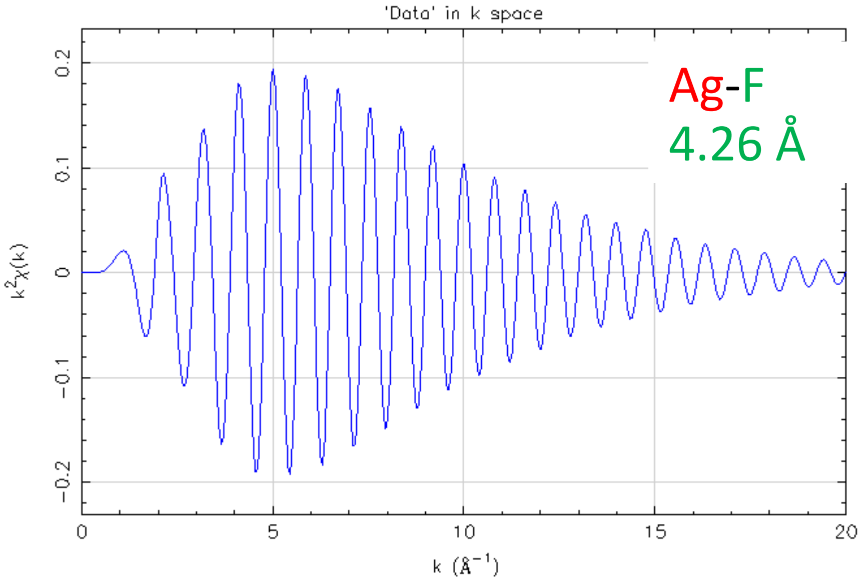

Scattering amplitude and phase shift: F(k) and δ(k)

The scattering amplitude F(k) and phase shift δ(k) depend on the atomic number

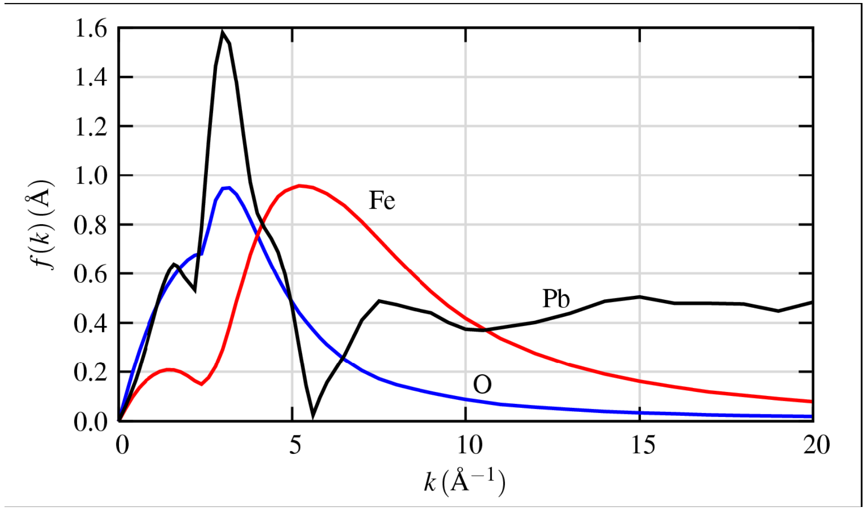

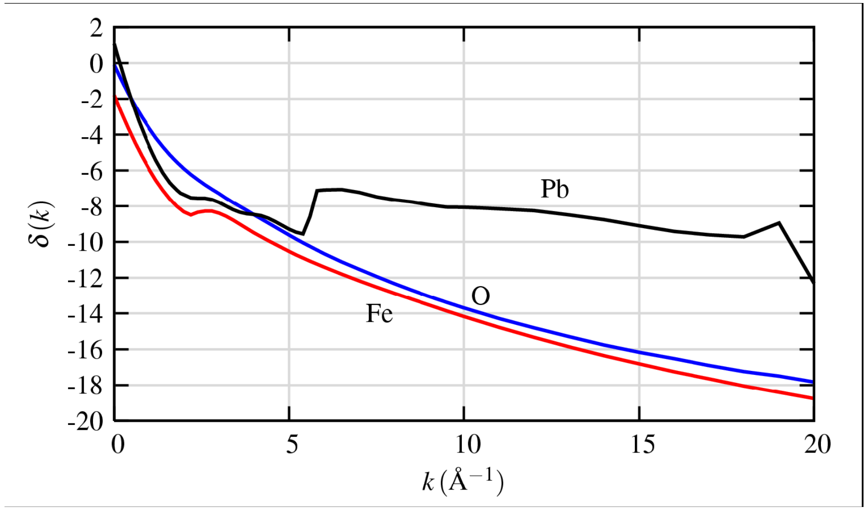

The scattering amplitude F(k) peaks at different k values and extends to higher k for heavier elements. For very heavy elements, there is structure in F(k).

The phase shift δ(k) shows sharp changes for very heavy elements.

These scattering functions can be accurately calculated and used in the EXAFS modeling

Z can usually be determined to within 5 or so. Fe and O can be distinguished, but Fe and Mn cannot

Multiple scattering

Multiple scattering events may occur

The photoelectron scatter from more than one atom before returning to the central atom

SS $\Rightarrow$ $g_2(r)$
$f = 2\ R_1$

MS $\Rightarrow$ $g_2(r)$
$f = 4\ R_1$

MS $\Rightarrow$ $g_3(r)$
$f = R_1 + R_2 + R_3$

MS $\Rightarrow$ $g_3(r)$
$f = 2R_1 + 2R_3$

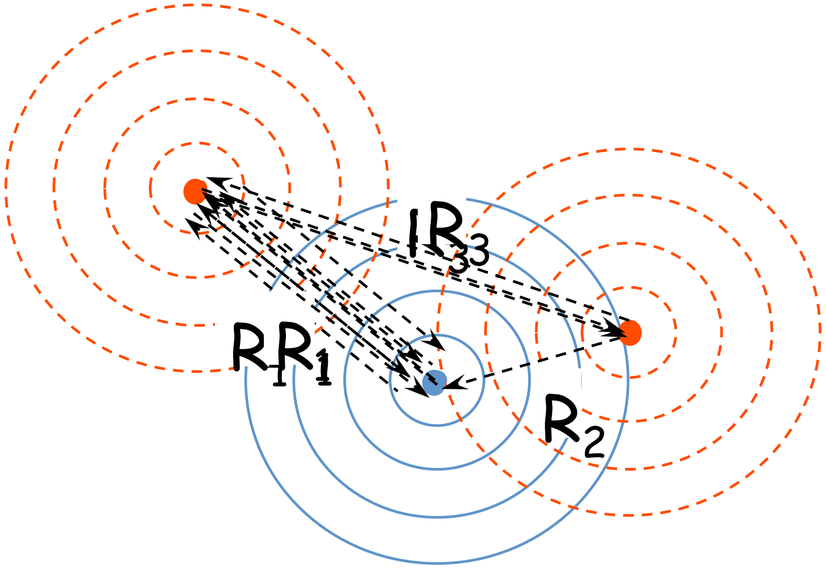

Through multiple scattering EXAFS can give information on the n-body distribution functions $g_n(r)$

Qualitative picture of local coordination in R space

The frequencies contained in the EXAFS signal depend on the distance between the absorbing atom and the neighbouring atoms (i.e. the length of the scattering path).

A Fourier Transform of the EXAFS signal provides a photoelectron scattering profile as a function of the radial distance from the absorber.

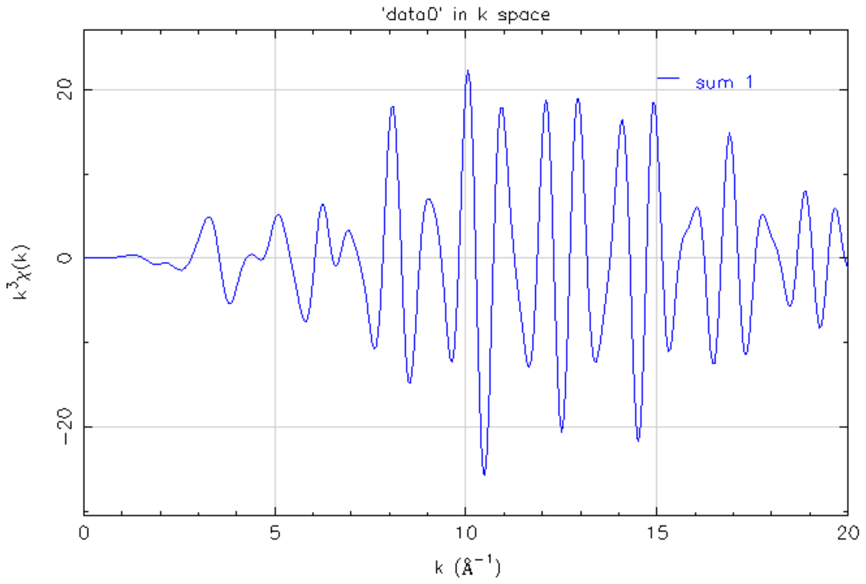

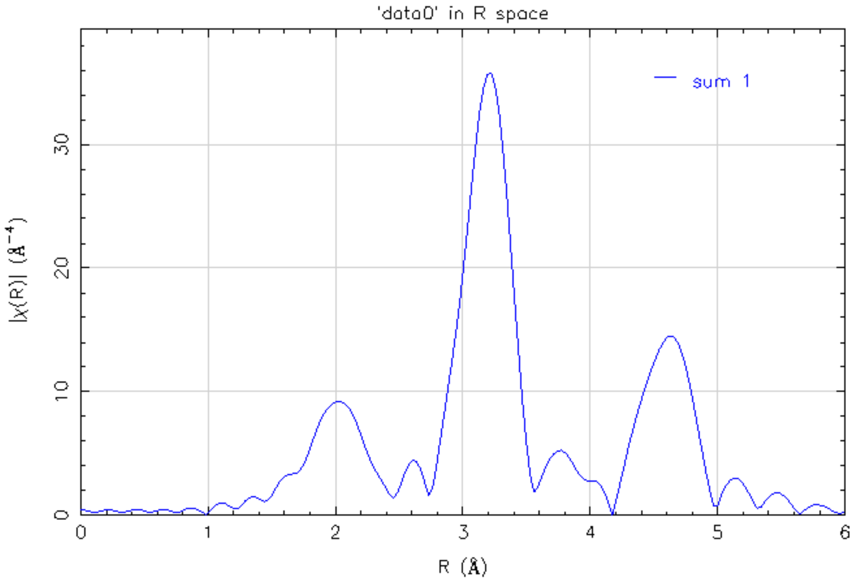

Quantitative structural determination

Structural determinations depend on the feasibility of resolving the data into individual waves corresponding to the different types of neighbours (SS) and bonding configurations (MS) around the absorbing atom

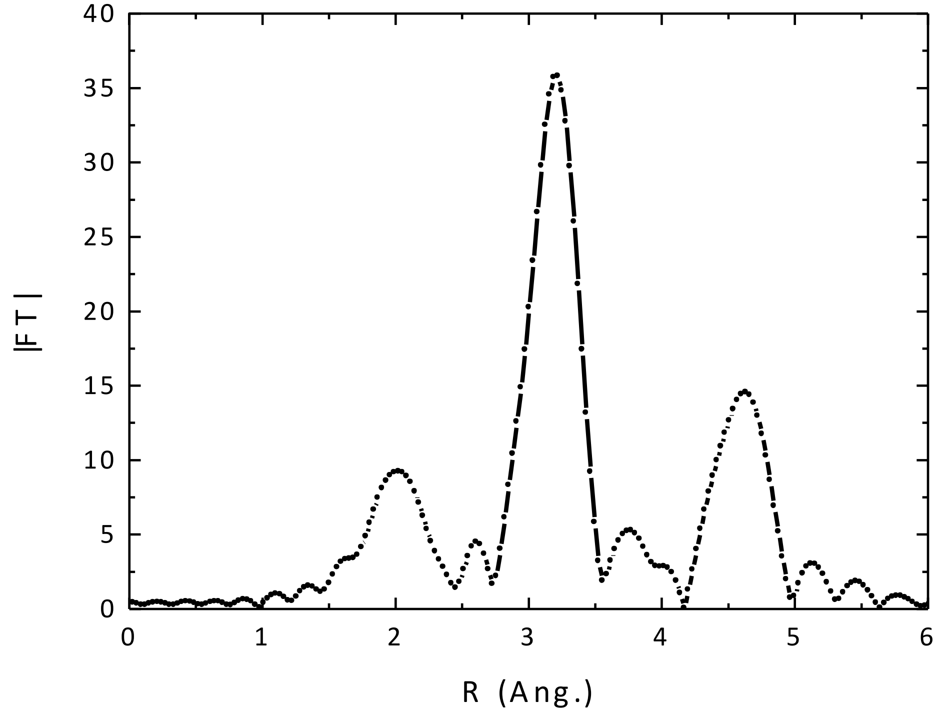

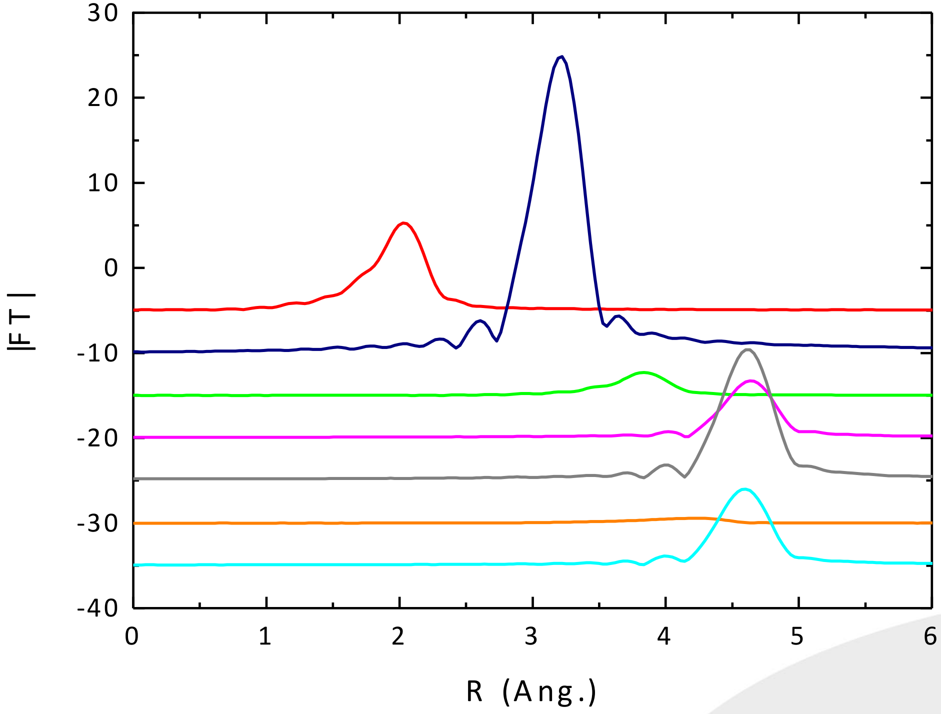

giuliana.aquilanti@elettra.eu

XAS vs diffraction methods

Diffraction Methods (x-rays, Neutrons)

- Crystalline materials with long-range ordering -> 3D picture of atomic coordinates
- Materials with only short-range order (amorphous solid, liquid, or solution) -> 1D RDF containing interatomic distances due to all atomic pairs in the sample

XAFS

- 1D radial distribution function (centered at the absorber)
- Element selectivity
- Higher sensitivity to local distortions (i.e. within the unit cell)
- Charge state sensitivity (XANES)
- Structural information on the environment of each type of atom:
    - distance, number, kind, static and thermal disorder
    - 3-body correlations

giuliana.aquilanti@elettra.eu

EXAFS: typical applications

Element selectivity

Local structure sensitivity

- Local structure in non-crystalline matter
- Local environment of an atomic impurity in a matrix of different atomic species
- Study of systems whose local properties differ from the average properties
- Detection of very small distortions of local structure

Outline

- X-ray absorption
- X-ray absorption fine structure
- XANES
- Some examples of EXAFS and XANES studies for cultural heritage

XANES

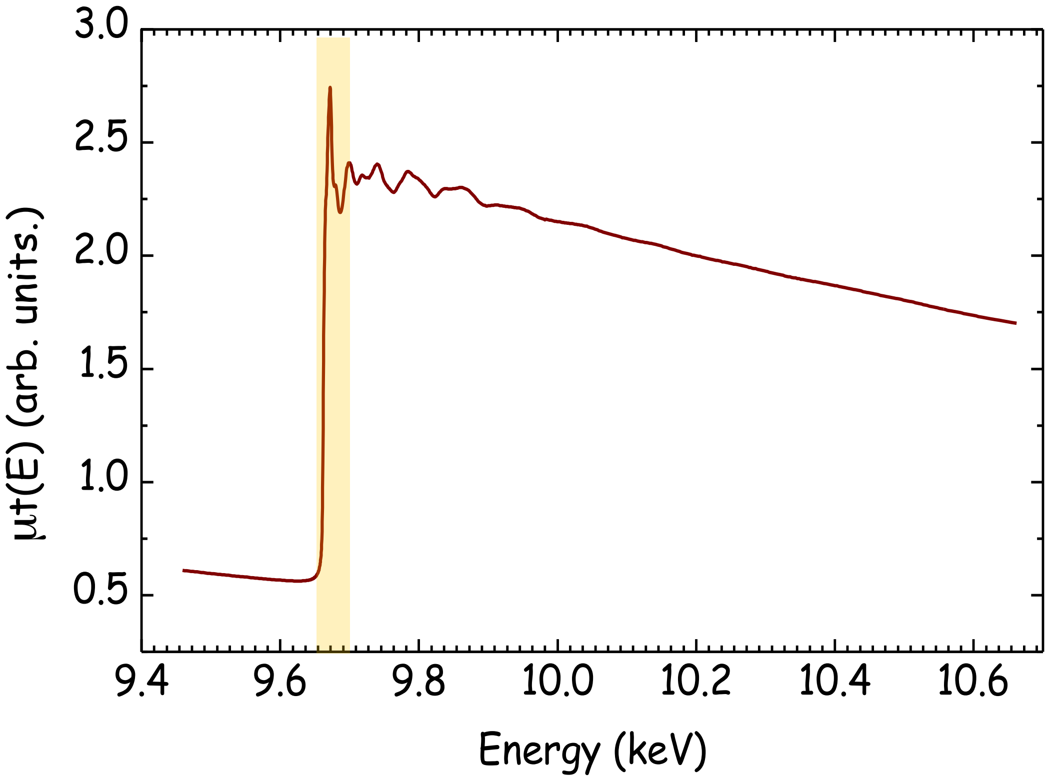

XANES is the region of the absorption spectrum within ~ 60 eV of the absorption edge

X-ray
Absorption
Near
Edge
Structure

XANES includes also the "pre-edge features" if any

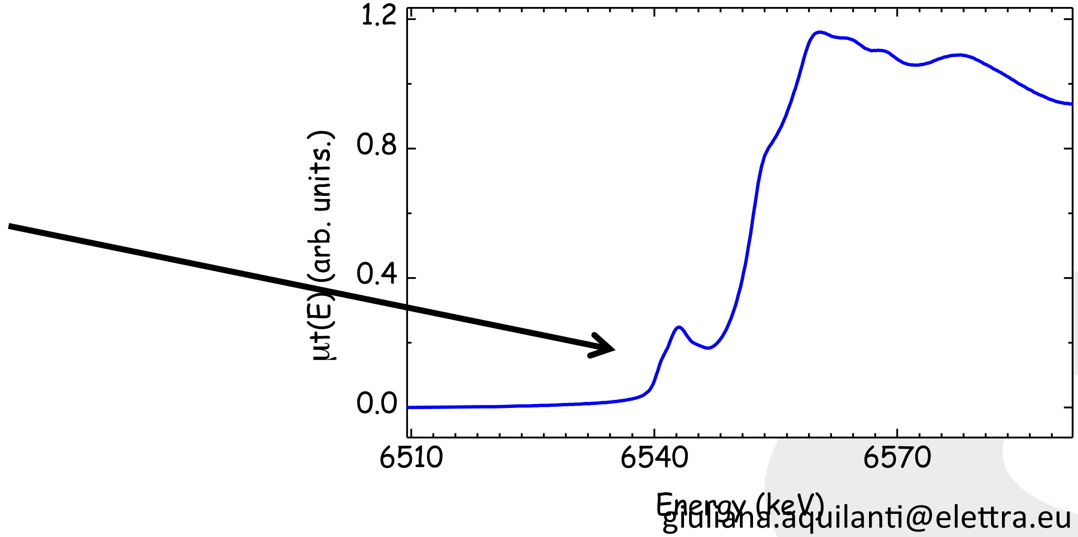

giuliana.aquilanti@elettra.eu

K-edge XANES

Mn: [Ar] $3d^5 4s^2$

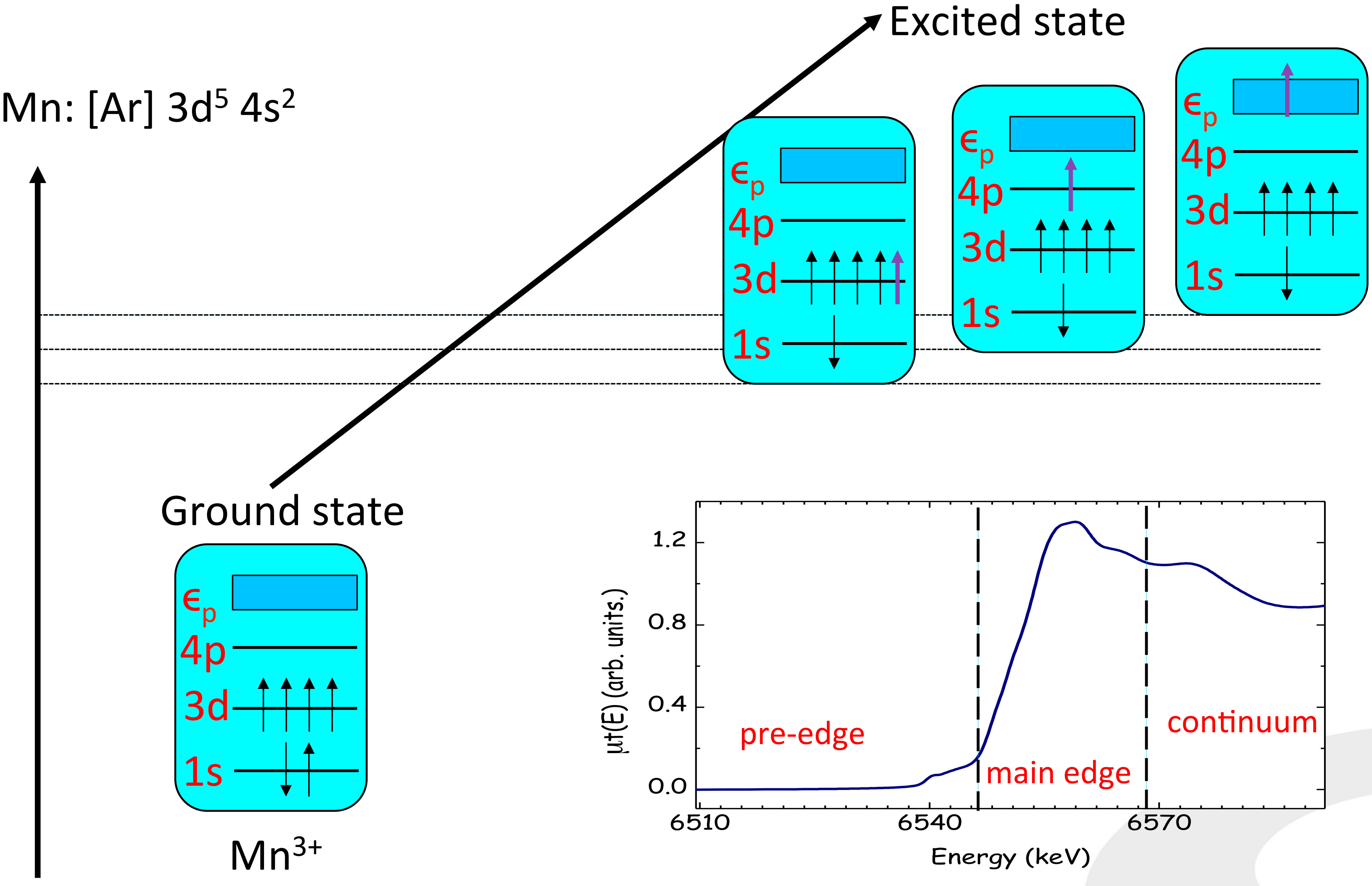

Chemical shift

Mn: [Ar] $3d^5\ 4s^2$

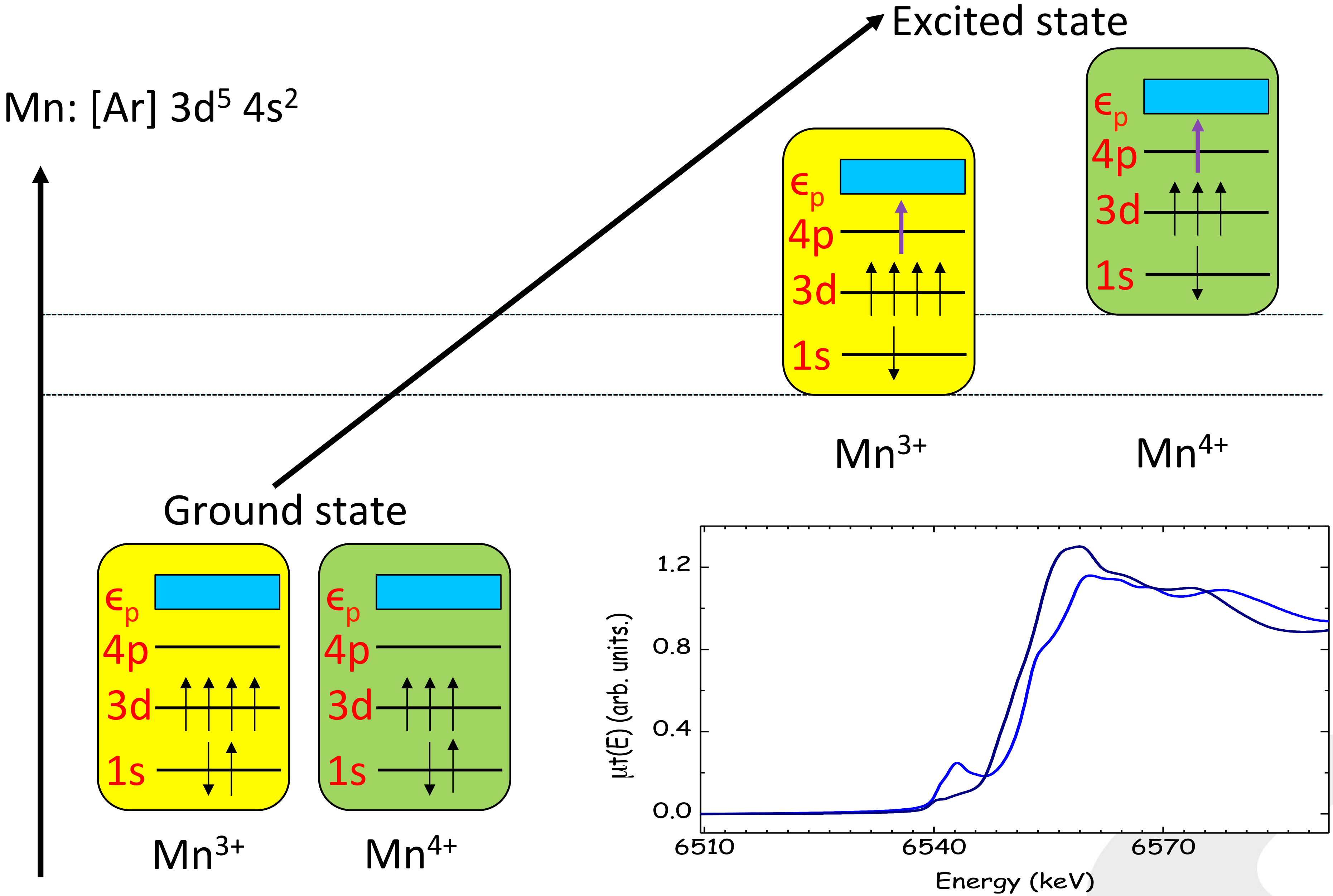

Excited state

Ground state

Mn^{3+} Mn^{4+}

giuliana.aquilanti@elettra.eu

Edge position: oxidation state - 1

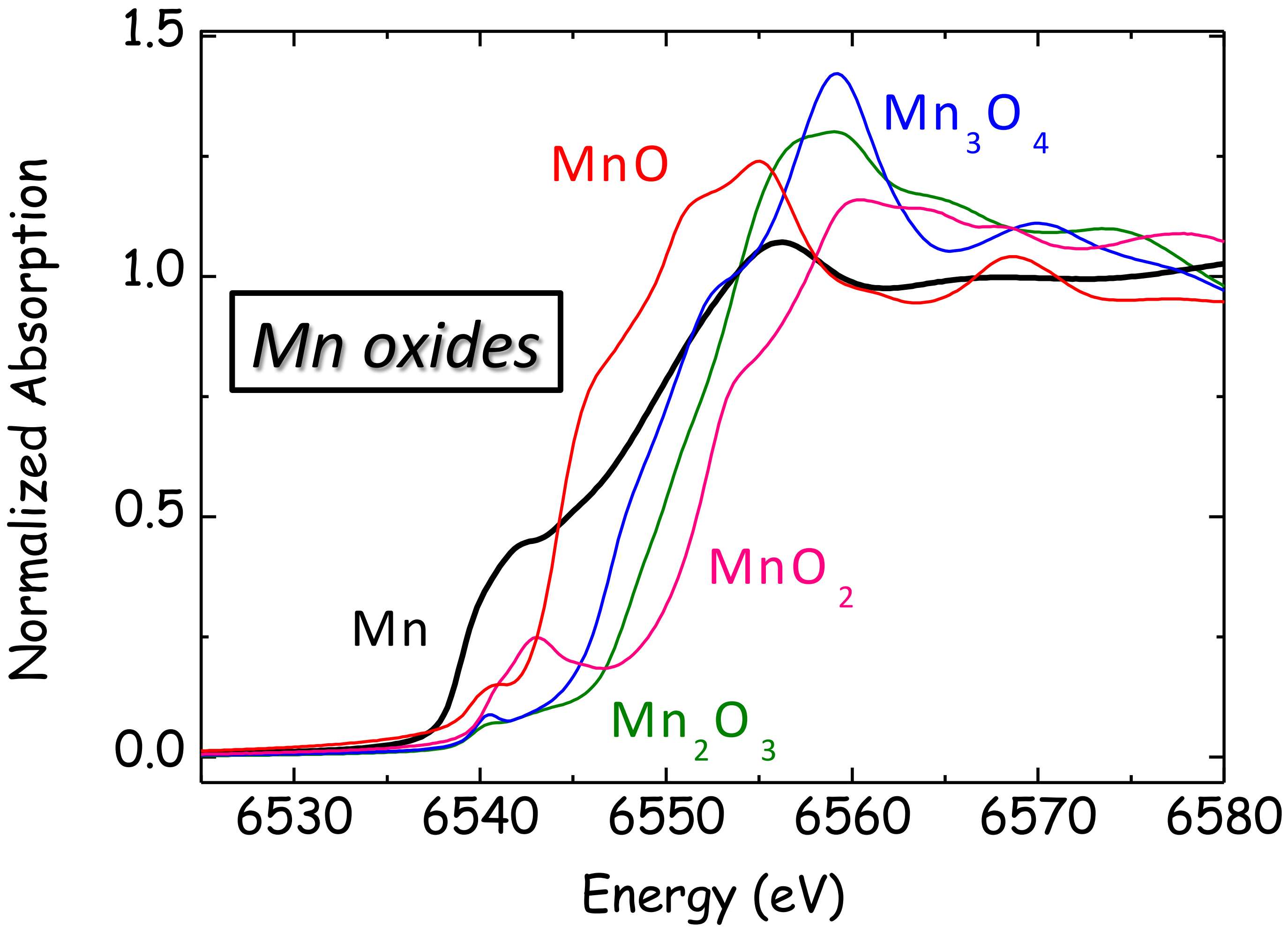

The edges of many elements show significant edge shifts (binding energy shifts) with oxidation state.

giuliana.aquilanti@elettra.eu

Edge position: oxidation state - 2

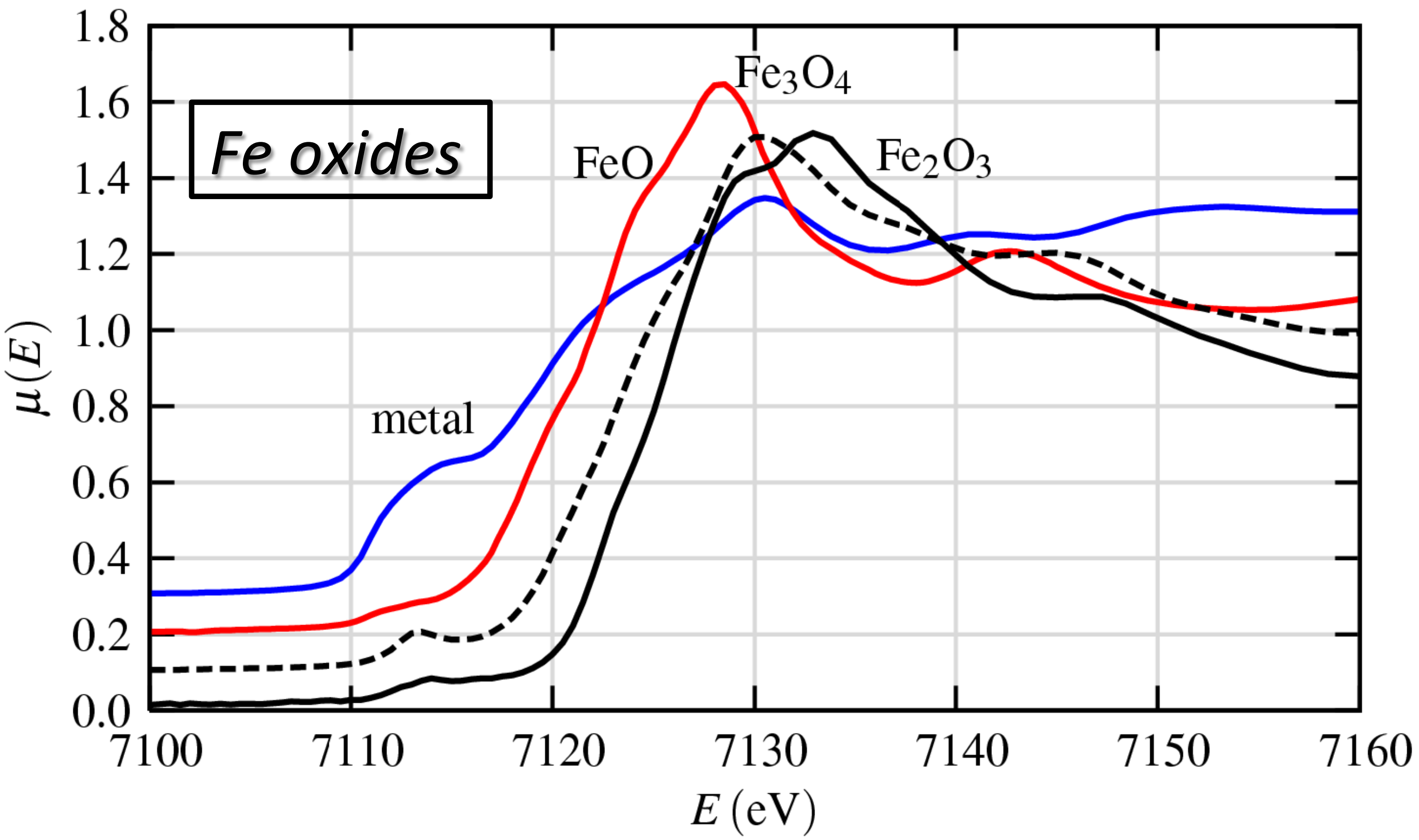

The heights and positions of pre-edge peaks can also be reliably used to determine Fe^{3+}/Fe^{2+} ratios (and similar ratios for many cations)

Edge position: oxidation state - 3

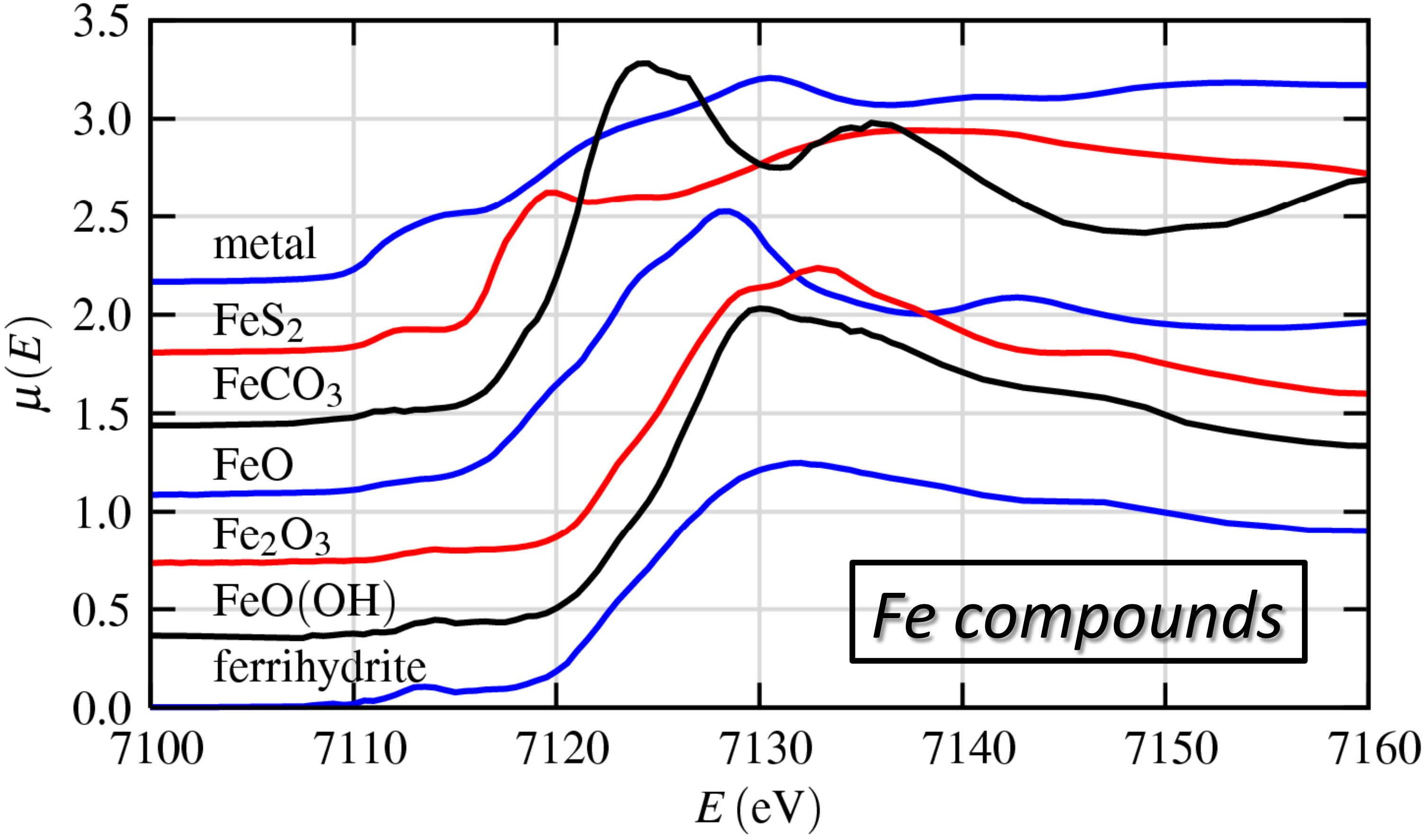

XANES can be used simply as a fingerprint of phases and oxidation state

XANES analysis can be as simple as making linear combinations of “known” spectra to get compositional fraction of these components

XANES transition

Dipole selection rules apply:

$$\boxed{\begin{aligned} \Delta\ell &= \pm 1 \\ \Delta s &= 0 \\ \Delta j &= \pm 1, 0 \\ \Delta m &= 0 \end{aligned}}$$

EDGE	INITIAL STATE	FINAL STATE
K, L_1	s (ℓ=0)	p (ℓ=1)
L_2, L_3	p (ℓ=1)	s (ℓ=0), d (ℓ=2)

The final state is usually not atomic-like and may have mixing (hybridization) with other orbitals.

This is often the interesting part of the XANES

giuliana.aquilanti@elettra.eu

Transition metals pre-edge peaks

Transition from 1s to 4p states

Pure octahedron

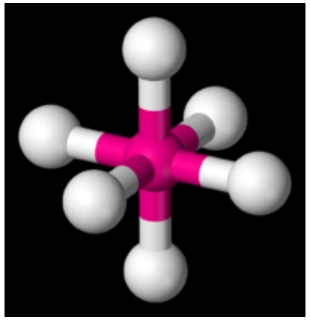

- Centro-symmetry: no p-d mixing allowed
- Only (weak) quadrupolar transitions
- No, or very low intensity prepeak

Distorted octahedron

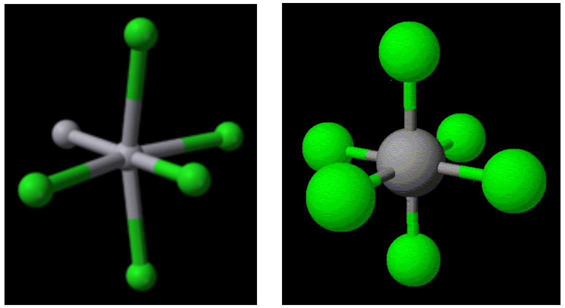

- Centro-symmetry broken: p-d mixing allowed
- Dipole transition in the edge
- Moderate intensity prepeak

Tetrahedron

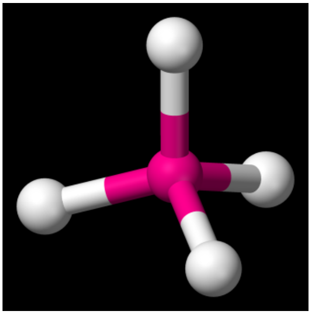

- No centro-symmetry : p-d mixing allowed
- Dipole transition in the edge
- High intensity prepeak

Prepeak: local coordination environment

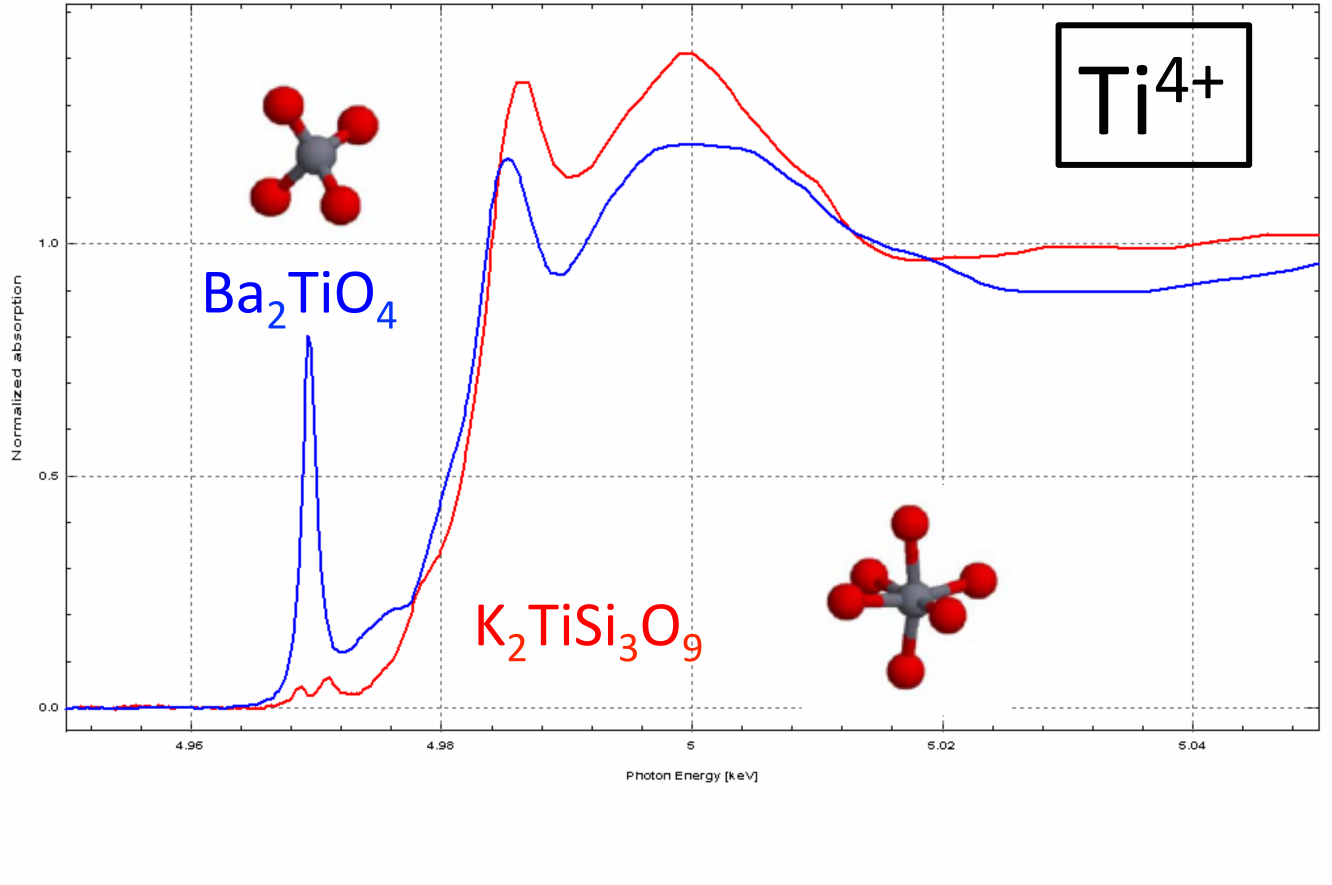

Ti K-edge XANES shows dramatic dependence on the local coordination chemistry

Pre-peak : oxidation state

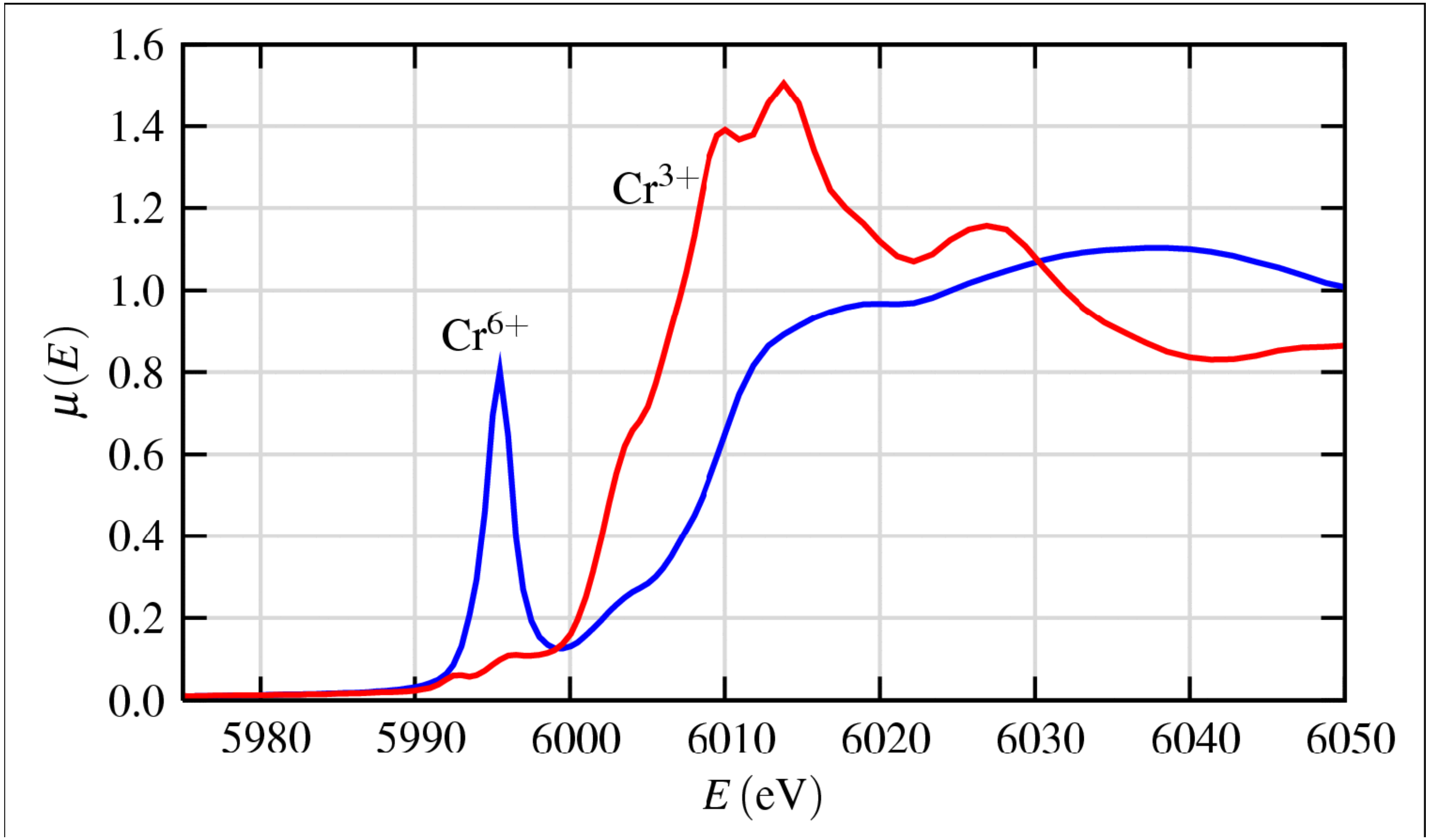

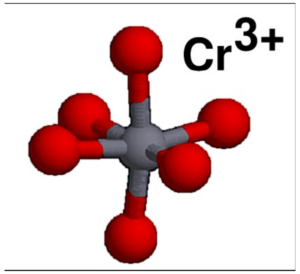

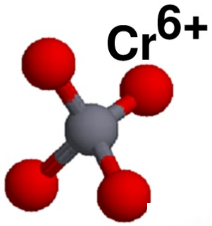

The XANES of Cr^{3+} and Cr^{6+} shows a dramatic dependence on oxidation state and coordination chemistry.

giuliana.aquilanti@elettra.eu

White line intensity of L_3-edge of XANES of 4d metals

Transition from $2p_{3/2}$ to 4d states

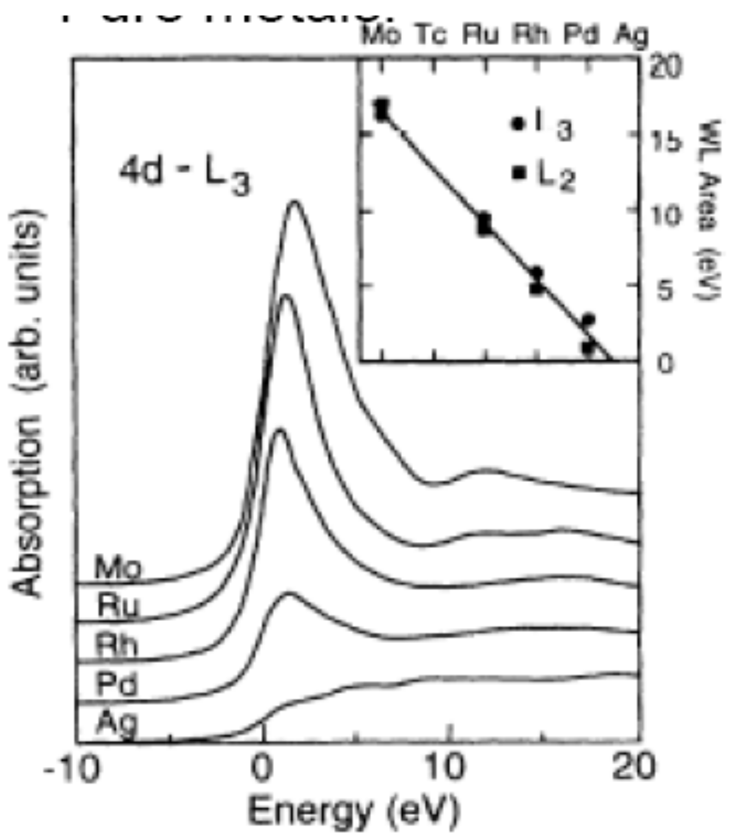

Linear correlation between white line area and number of 4d-holes for Mo to Ag

Increasing d states
occupancy

White line intensity: oxidation state

Re L_3-edge: transition from $2p_{3/2}$ to 5d states

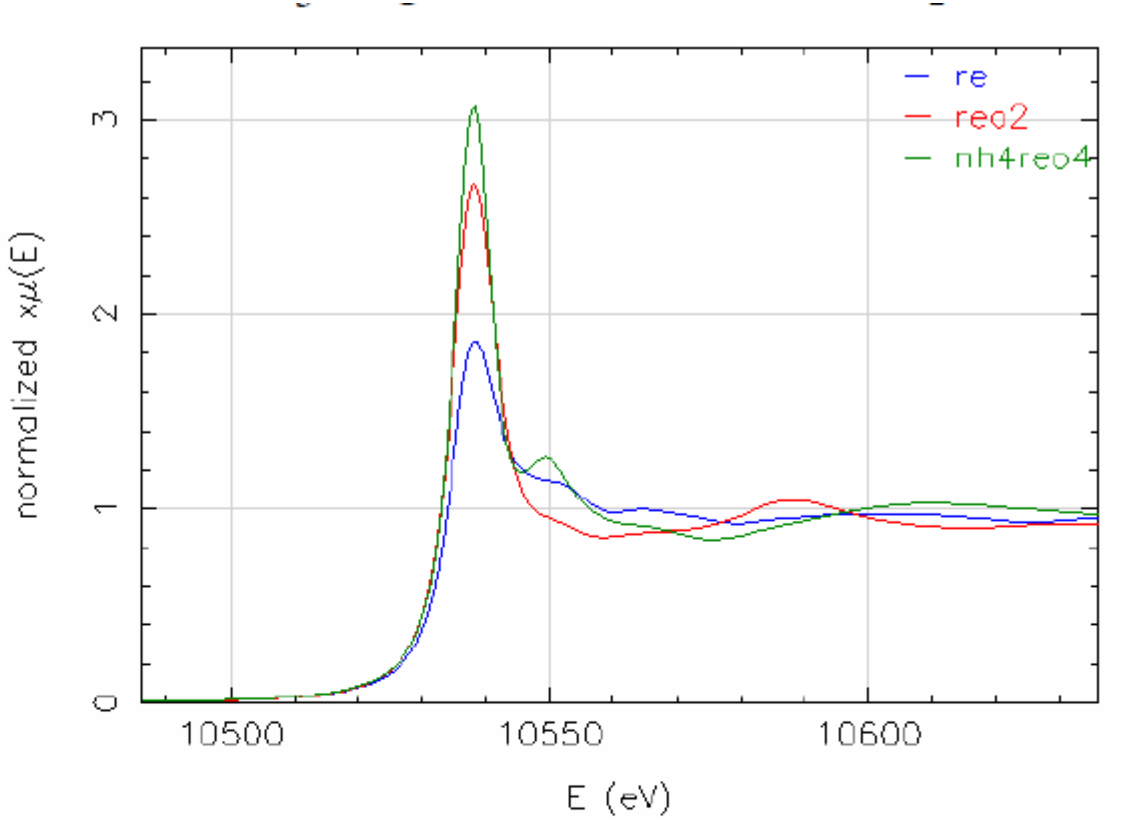

Re metal (Re^0) – $5d^5$

ReO_2 (Re^{4+}) – $5d^1$

NH_4ReO_4 (Re^{7+}) $5d^0$

giuliana.aquilanti@elettra.eu

Elettra
Sincrotrone
Trieste

XANES: interpretation

The EXAFS equation breaks down at low-k, and the mean-free-path goes up.

This complicates XANES interpretation:

A simple equation for XANES does not exist

XANES can be described *qualitatively* (and nearly *quantitatively*) in terms of:

- Coordination chemistry: regular, distorted octahedral, tetrahedral, . . .
- Molecular orbitals: p-d orbital hybridization, crystal-field theory, . . .
- Band-structure: the density of available electronic states
- Multiple-scattering: multiple bounces of the photoelectron

giuliana.aquilanti@elettra.eu

XANES: conclusions

XANES is a much larger signal than EXAFS

- XANES can be done at lower concentrations, and less-than-perfect sample conditions

XANES is easier to crudely interpret than EXAFS

- For many systems, the XANES analysis based on linear combination of known spectra form "model compounds" is sufficient

XANES is harder to fully interpret than EXAFS

- The exact physical and chemical interpretation of all spectral features is still difficult to do accurately, precisely, and reliably.

giuliana.aquilanti@elettra.eu

Outline

- X-ray absorption
- X-ray absorption fine structure
- XANES
- Some examples of EXAFS and XANES studies for cultural heritage

giuliana.aquilanti@elettra.eu

General statement

XAFS spectroscopy is a potentially very useful technique to be applied in Cultural Heritage studies

- It is a non-destructive method which can be applied in air
- It virtually does not require any restriction on the type and size of the sample (metal, ceramic, glass, cloth, paper, etc.)
- It is applicable to most of the elements of interest, even in very low concentration

All these characteristics are particularly important in archaeological applications, in which samples are precious cultural heritage made of very different materials.

giuliana.aquilanti@elettra.eu

Chromophores and pigments

- The chromatic response of a pigment is linked to the symmetry, valence state and local geometry of the chromophore (usually a 3d metal)
- The color is also influenced by the oxidation state of the metal cation
- In general metals were added to production or painting materials with the aim of giving a particular hue to the manufact but they are present in limited amount, typically below 1 at% (fluorescence mode detection)

giuliana.aquilanti@elettra.eu

Elettra
Sincrotrone
Trieste

Fe and Mn K-edge XANES study of ancient Roman glasses

- Study of ancient glasses from Patti Roman Villa (Messina, Sicily)
- From the chemical point of view, the samples are 'low-magnesia' glasses, with a composition typical of the Roman period
- Glasses of different colors from light green to pale brown
- Fe and Mn K-edge XANES

Aim of the work

- To test the influence of iron oxidation state on the color of the studied samples
- To identify the possible decolorant role of manganese oxide in the almost uncolored samples

S. Quartieri et al., Eur. J. Min. (2002) 14(4),749-756

giuliana.aquilanti@elettra.eu

Fe and Mn K-edge XANES study of ancient Roman glasses

Fragments of perfume bottles (2nd century AD)

S. Quartieri et al., Eur. J. Min. (2002) 14(4),749-756

Fe and Mn K-edge XANES study of ancient Roman glasses

Glass A: pale green

Glass B: uncolored

Glass C: pale brown

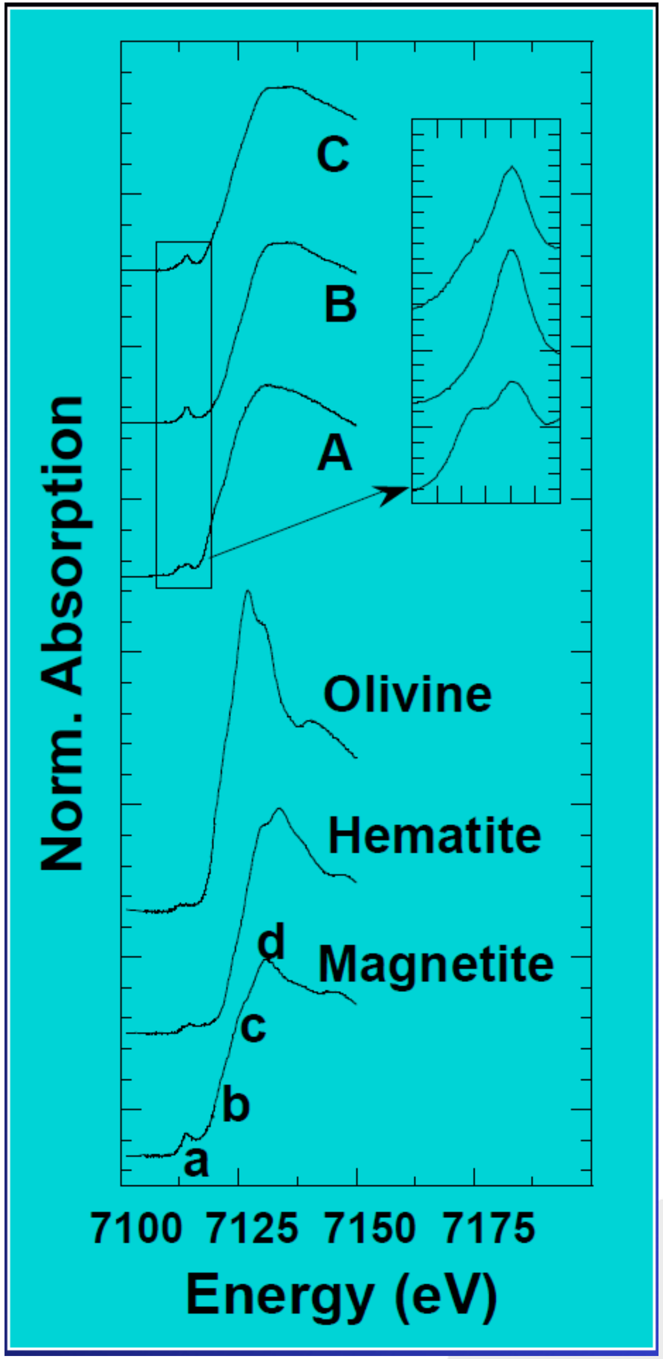

- B and C similar to each other: both in the general Shape and in the energy position of the different features
- Features (b) and (d) fall at high energy characteristic of Fe^{3+}

S. Quartieri et al., Eur. J. Min. (2002) 14(4),749-756

Fe and Mn K-edge XANES study of ancient Roman glasses

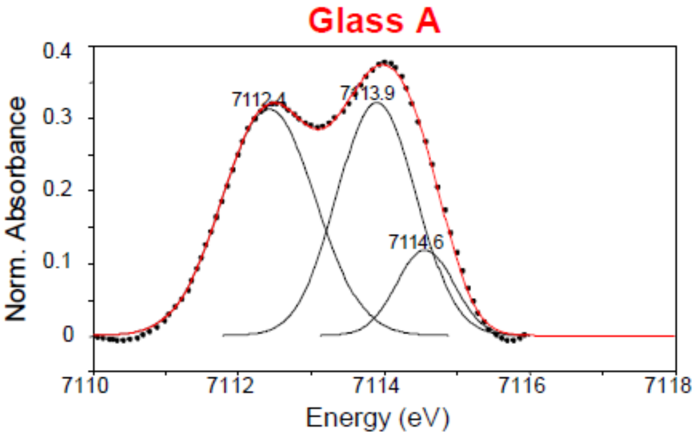
Glass A

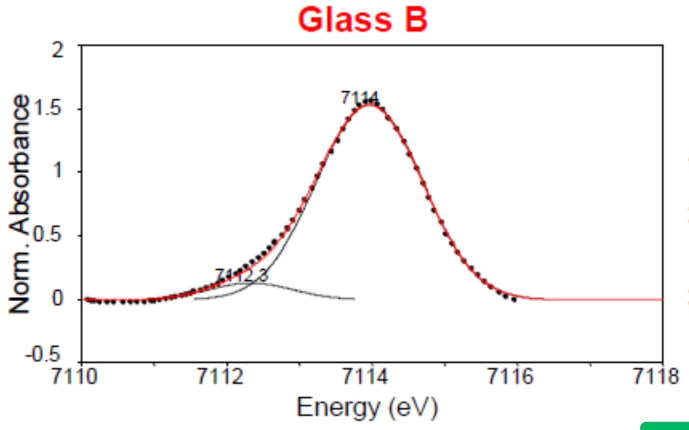
Glass B

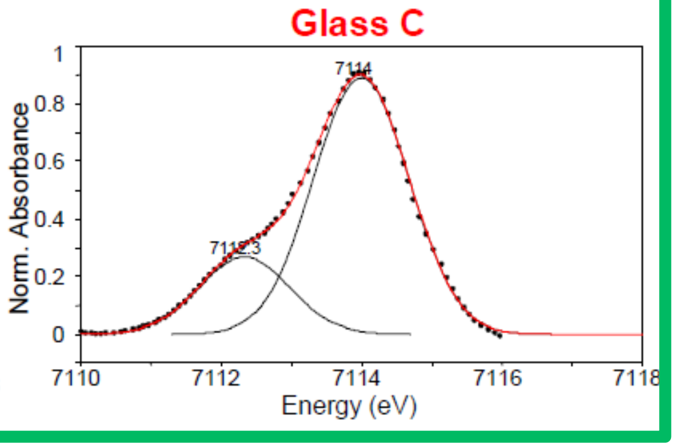
Glass C

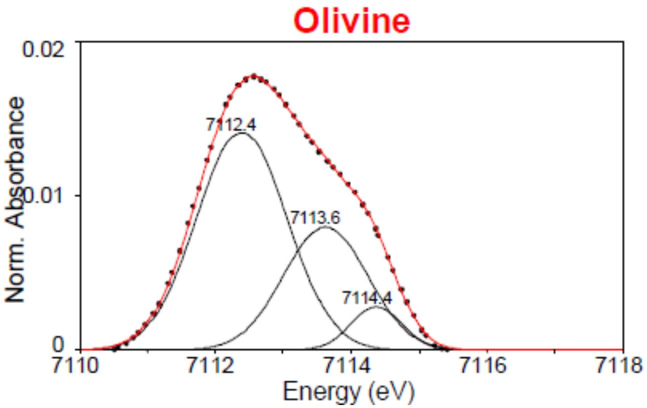
Olivine

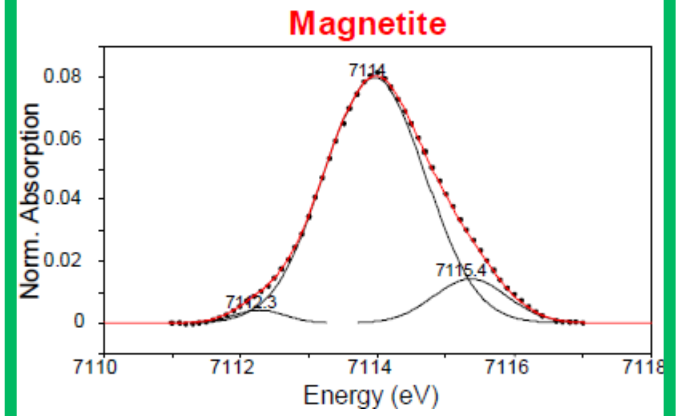
Magnetite

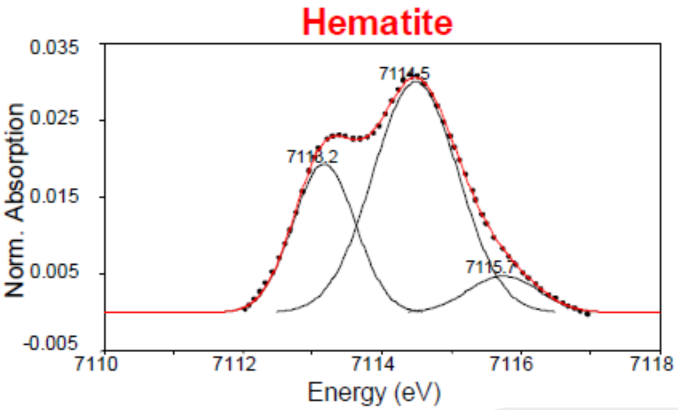
Hematite

S. Quartieri et al., Eur. J. Min. (2002) 14(4),749-756

Fe and Mn K-edge XANES study of ancient Roman glasses

Glass A: pale green

Glass B: uncolored

Glass C: pale brown

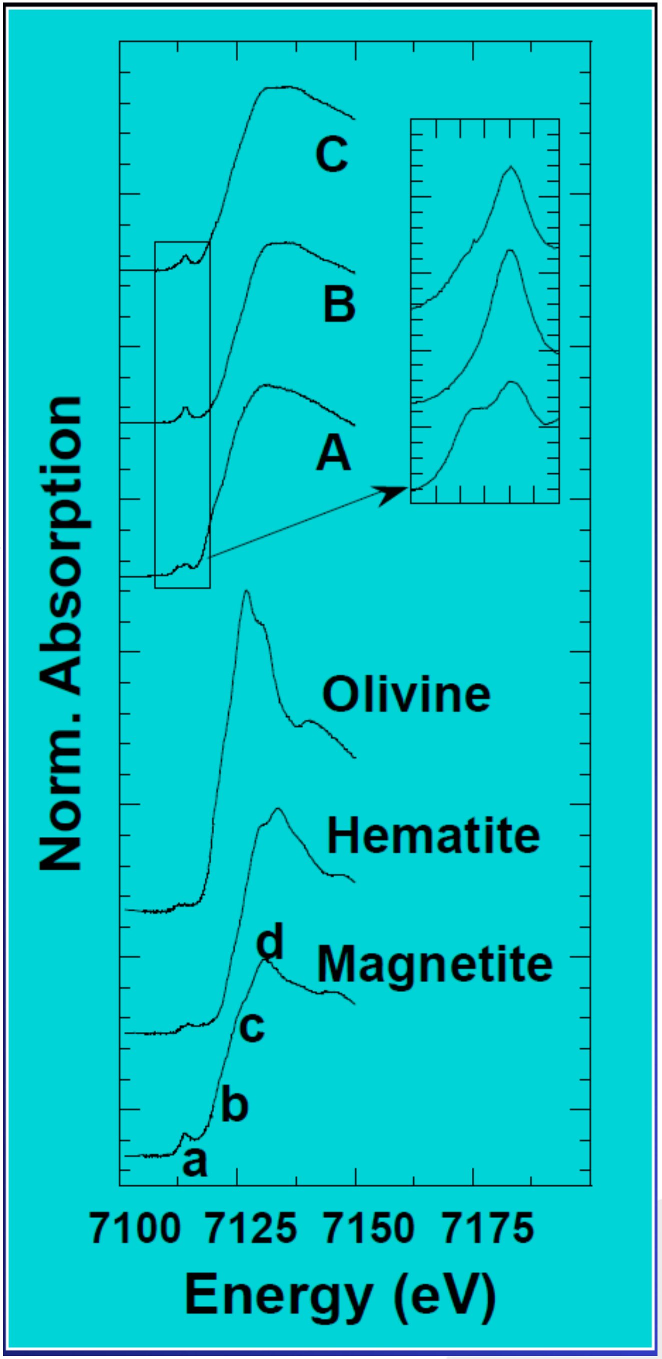

- In sample A the features (b) and (d) are at much lower energy, nearer to those present in the olivine spectrum characteristic of Fe^{+2}

S. Quartieri et al., Eur. J. Min. (2002) 14(4),749-756

Fe and Mn K-edge XANES study of ancient Roman glasses

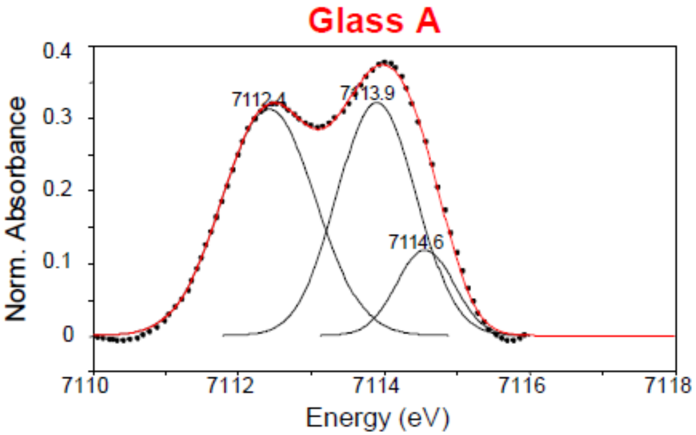
Glass A

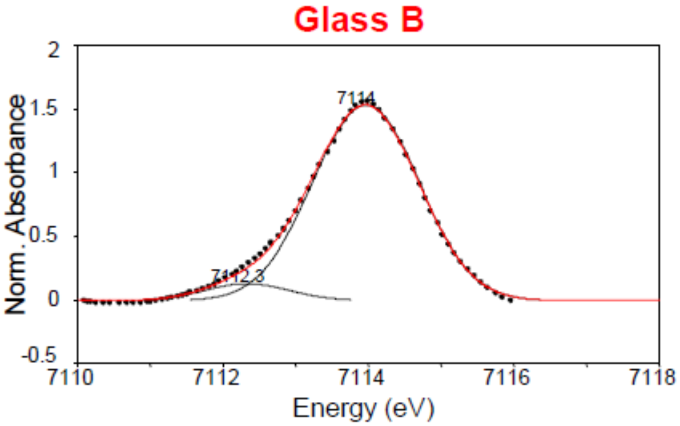
Glass B

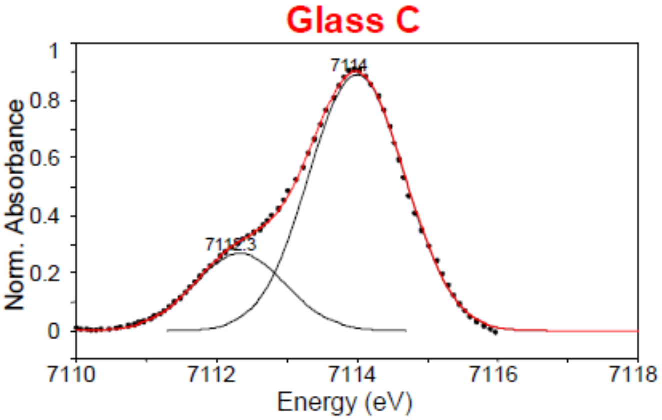
Glass C

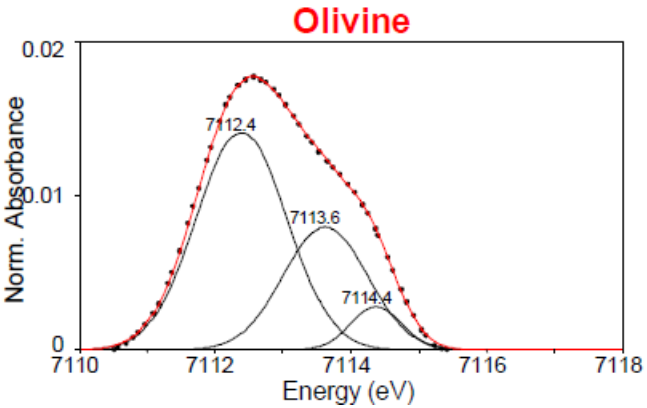
Olivine

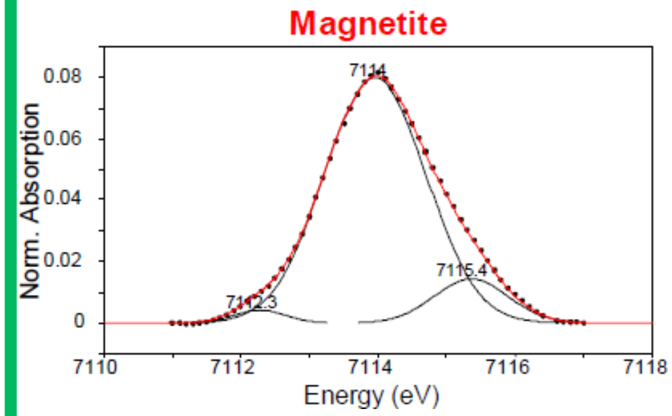
Magnetite

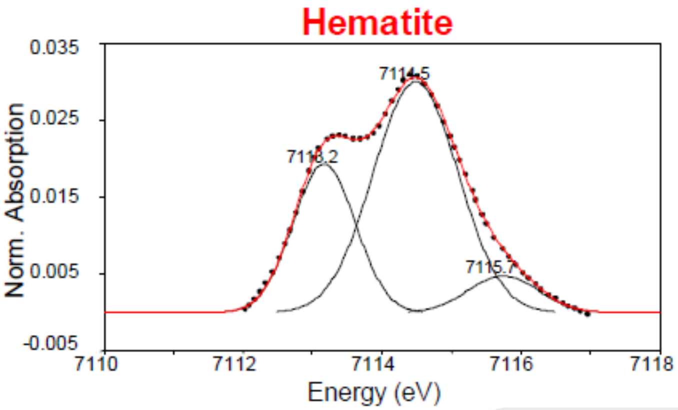
Hematite

S. Quartieri et al., Eur. J. Min. (2002) 14(4),749-756

Fe and Mn K-edge XANES study of ancient Roman glasses

Glass A: pale green
Glass B: uncolored
Glass C: pale brown

- In glass C and in glass B, Fe is predominantly in 3+ oxidation state
- In glass A there is a high percentage of Fe^{2+}

S. Quartieri et al., Eur. J. Min. (2002) 14(4),749-756

giuliana.aquilanti@elettra.eu

Fe and Mn K-edge XANES study of ancient Roman glasses

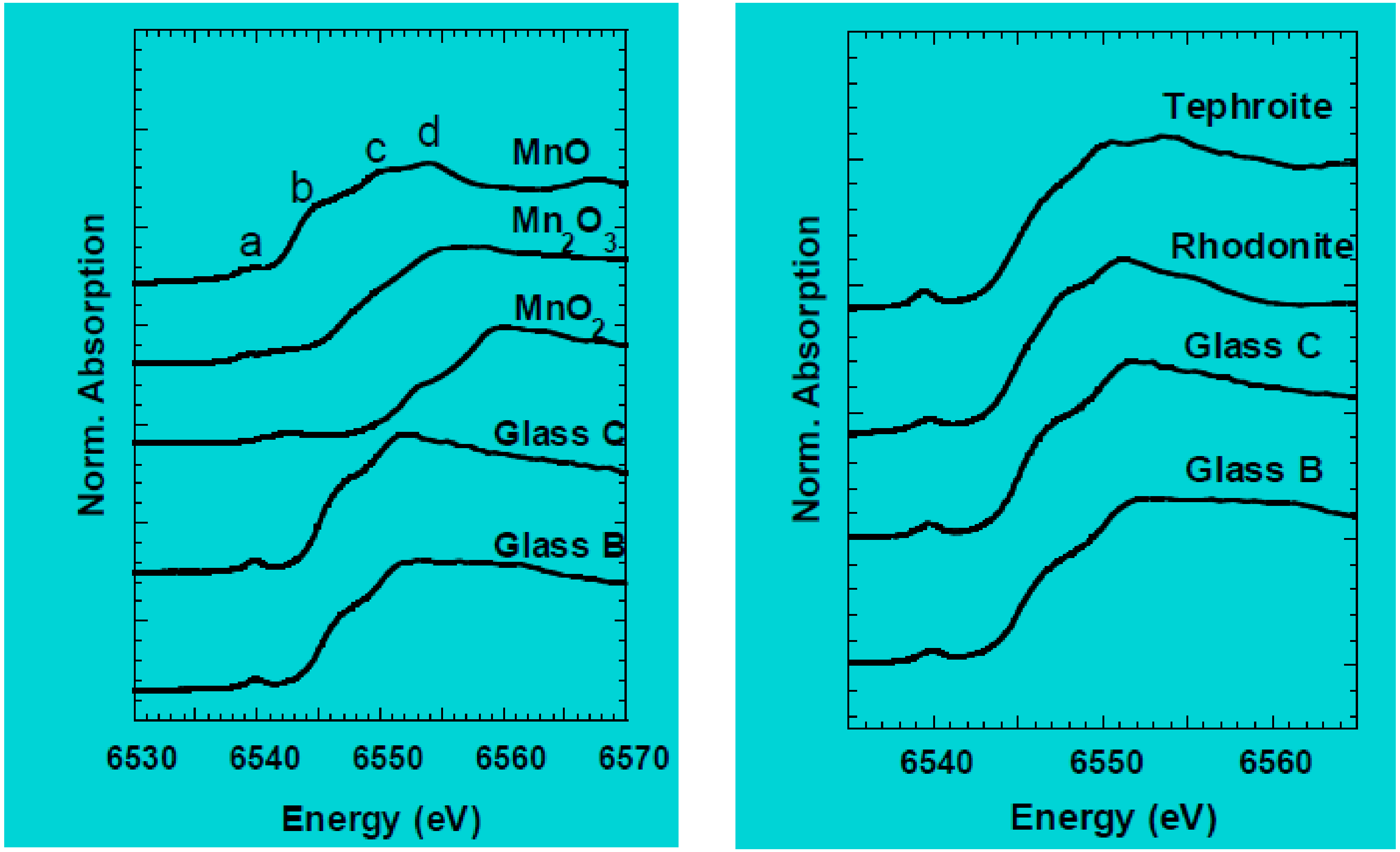

- Mn is in reduced form
- Strong similarity between the two Mn^{2+}-silicatic reference compounds

giuliana.aquilanti@elettra.eu

Fe and Mn K-edge XANES study of ancient Roman glasses

Glass A: pale green
Glass B: uncolored
Glass C: pale brown

Conclusion

- In sample B and C, Mn^{4+} has oxidised Fe^{2+} to Fe^{3+} and therefore is present in the reduced form
- It is confirmed the hypothesis of a redox interaction between manganese and iron as a results of a deliberate addition of pyrolusite (mineral containing MnO_2) – reported in literature as the main decolorant in the Roman period – during the melting procedure of the uncolored glass

S. Quartieri et al., Eur. J. Min. (2002) 14(4),749-756

giuliana.aquilanti@elettra.eu

A bit of history

Maiolica is Italian tin-glazed pottery dating from the Renaissance

The very earliest examples of maiolica date back to 9th century in Mesopotamia. In the 11th century, Islamic ceramicists were creating richly detailed lustre decorated pieces

Thin metallic film containing silver, ***copper*** *and other substances, like iron oxide and cinnabar, applied in a reducing atmosphere on a previously glazed ceramic.*

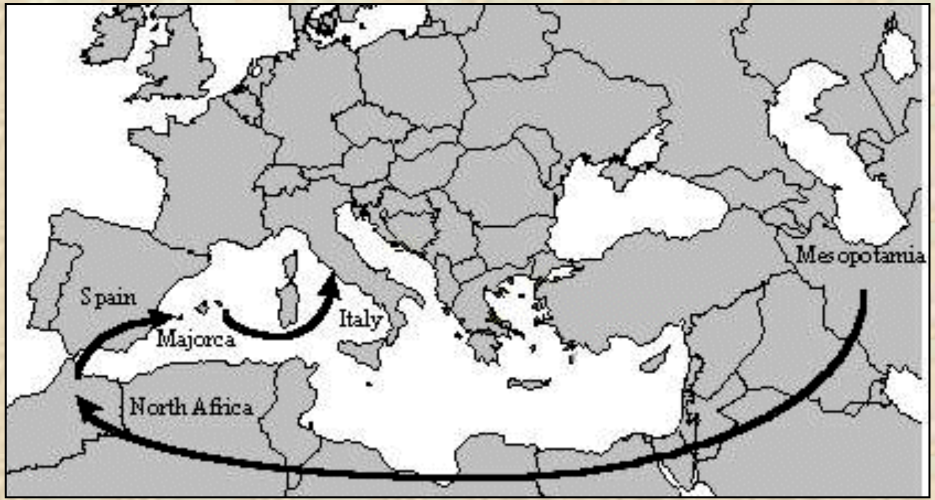

By the 13th century traders were importing majolica into Italy through the Isle of Majorca. Therefore the italian called this new type of ceramic Maiolica, regardless of its place of origin.

C. Guglieri Rodriguez et al., J. Anal. At. Spectrom., 2015,30, 738

XAS studies of Italian and Hispano-Moorish Majolicas

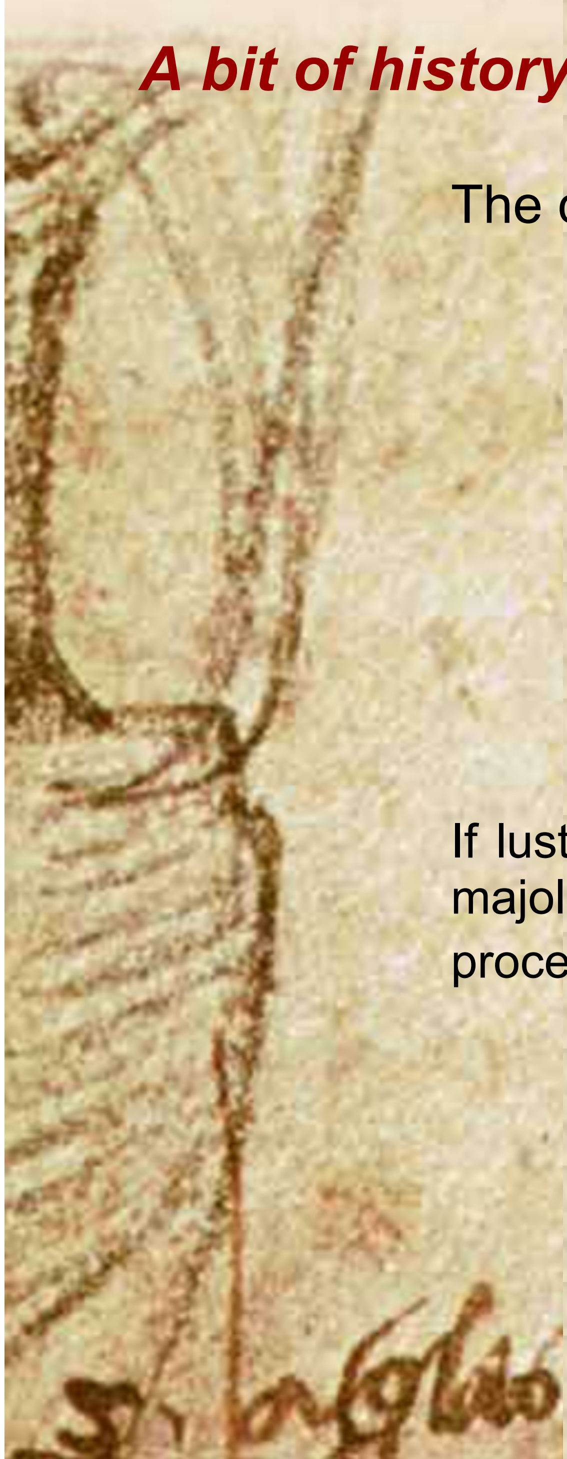

A bit of history

The creation of Maiolica is a complex “Five-Step” process

-First firing (about 1000 °C)

-Glazing (inmersion on a mix of sand, potassium carbonate, salts and oxides, such as lead and tin oxides, with water)

-Painting the glazed surface

-Second firing at 900 °C

If lustre: extra step needed to achieve the reflections and iridescences on majolica. A third firing in very complex conditions was the key of the process.

The local artisans became keepers of refined and secret recipes and techniques for decorating ceramic objects.

C. Guglieri Rodriguez et al., J. Anal. At. Spectrom., 2015,30, 738

XAS studies of Italian and Hispano-Moorish Majolicas

A bit of history

Dish with bird, in Islamic-derived style,
Arcaic ceramic, Orvieto.1270-1330

Italian potters began to create their own maiolica, firstly by coping the Spanish and Islamic designs, then mixing and adding their very own

C. Guglieri Rodriguez et al., J. Anal. At. Spectrom., 2015,30, 738

A bit of history

Dish with bird, in Islamic-derived style, Arcaic ceramic, Orvieto.1270-1330

Italian potters began to create their own maiolica, firstly by coping the Spanish and Islamic designs, then mixing and adding their very own

Indeed, a new style was developed, called istoriato, with lustre decoration, and representing the most beautiful Renaissance productions

Faenza, *istoriato* ware by Baldassare Manara, 1520

Dish from Deruta, 2nd quarter of the 16th

Istoriato charger, Feenza, 1555

During the late 15th and early 16th centuries: peak of artistic quality

C. Guglieri Rodriguez et al., J. Anal. At. Spectrom., 2015,30, 738

XAS studies of Italian and Hispano-Moorish Majolicas

Aim of this work

To investigate the chemical state and the local environment of metal atoms in the glaze, lustre and blue pigment, to understand the technological processes and materials in different production

Experiments: X-Ray absorption Spectroscopy

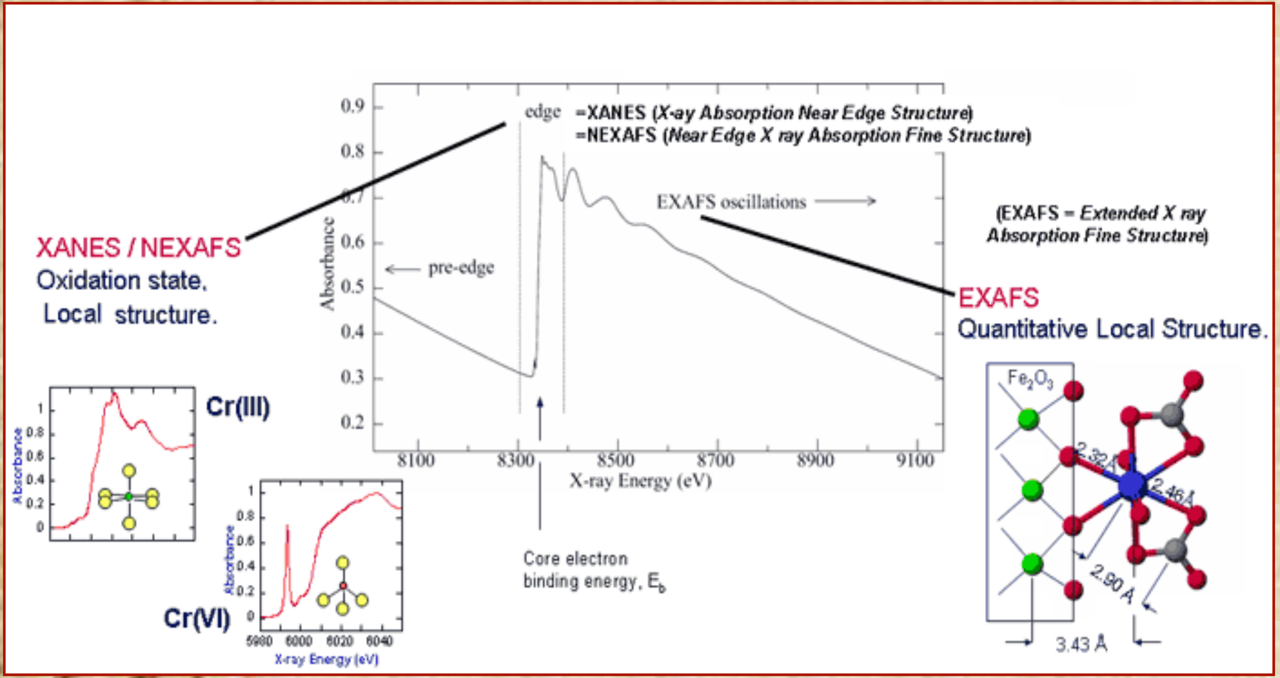

XAS measurements were performed on XAFS beamline, at Elettra Sincrotrone Trieste. A Si (111) double-crystal monochromator was used. The beam size was set at 1x1 mm2 and the photon flux was about 1010 photons/s. All spectra were collected at Fluorescence mode

http://www-ssrl.slac.stanford.edu/mes/remedi/index.html

C. Guglieri Rodriguez et al., J. Anal. At. Spectrom., 2015,30, 738

XAS studies of Italian and Hispano-Moorish Majolicas

Studied Maiolicas

Hispano-Moorish (LIM1) (s.XIII)

Blue decorated and lustred ceramic

L19 (s.XV)
Italian renaissance production

Blue decorated and lustred majolica

C. Guglieri Rodriguez et al., J. Anal. At. Spectrom., 2015,30, 738

XAS studies of Italian and Hispano-Moorish Majolicas

Analysis of the Lustre

*Lustre: Thin metallic film containing silver, **copper** and other substances, like iron oxide and cinnabar, applied in a reducing atmosphere on a previously glazed ceramic.*

↓

Cu K-edge

<ins>XANES</ins>

L19 → Cu^{1+}

LIM1 → Cu^{2+} indicating lower reduction state

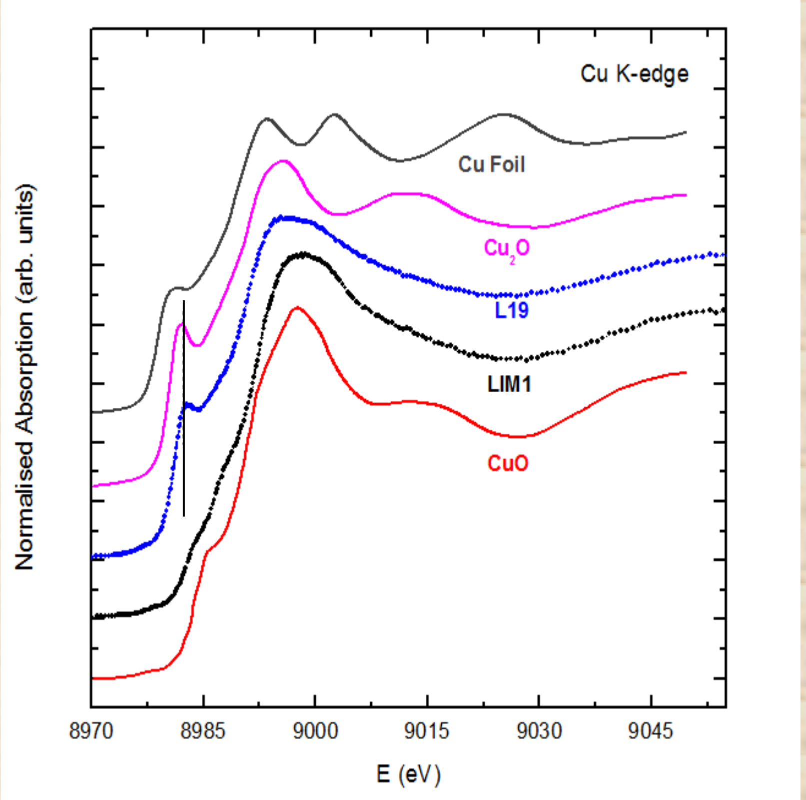

C. Guglieri Rodriguez et al., J. Anal. At. Spectrom., 2015,30, 738

XAS studies of Italian and Hispano-Moorish Majolicas

Analysis of the Lustre

Lustre: Thin metallic film containing silver, ***copper*** *and other substances, like iron oxide and cinnabar, applied in a reducing atmosphere on a previously glazed ceramic.*

↓

Cu K-edge

EXAFS

Just the contribution of the first Cu-O shell (amorphous)

Cu-O interatomic distance: at L19 are those of Cu_2O, at LIM1 those of CuO

Sample	Shell	N	r (Å)	σ^2 (Å^2)
CuO	Cu-O	4	1.95	
Cu_2O	Cu-O	2	1.84	
LIM1	Cu-O	3.5 ± 0.4	1.92 ± 0.01	0.006 ± 0.002
L19	Cu-O	3.2 ± 0.1	1.84 ± 0.01	0.005 ± 0.003

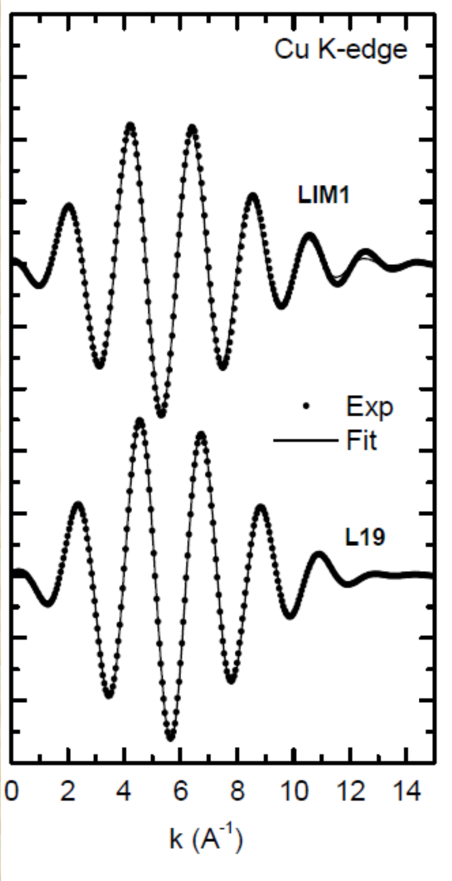

C. Guglieri Rodriguez et al., J. Anal. At. Spectrom., 2015,30, 738

Elettra
Sincrotrone
Trieste

Preservation of the XVII-century Warship VASA - 1

M. Sandstrom et al., *Nature*, 415, pp. 893–897, 2002.

- It sunk to a depth of 30 m in Stokholm harbour in 1628
- The salty and anaerobic conditions of the harbours water prevented wood-consuming plants, fauna or bacteria, from attacking the ship, thereby preserving the VASA in excellent conditions.
- It was raised in 1961 and after 30 years of preservation treatment was put on display in Stockholm in 1990.
- First problems detected in 2000
  - Crusty patches of salt in the surface
  - Softening of the woods
- XRD indicated the presence of sulphates (SO_4^-) and sulphur (S_8). It appeared that these materials were leaching out of solution from the bulk of the wood.

giuliana.aquilanti@elettra.eu

Elettra
Sincrotrone
Trieste

Preservation of the XVII-century Warship VASA - 2

- XANES had to be used instead of XRD because of the poor crystallinity of the sample and because of the spurious signals originating from the wood.
- The XANES spectra shows also intermediate oxidation state of sulphur, corresponding to the overall oxidation state reaction to sulphuric acid.

$$S(s) + \frac{3}{2}O_2 + H_2O \rightarrow 2H^+(aq) + {SO_4}^{2-}$$

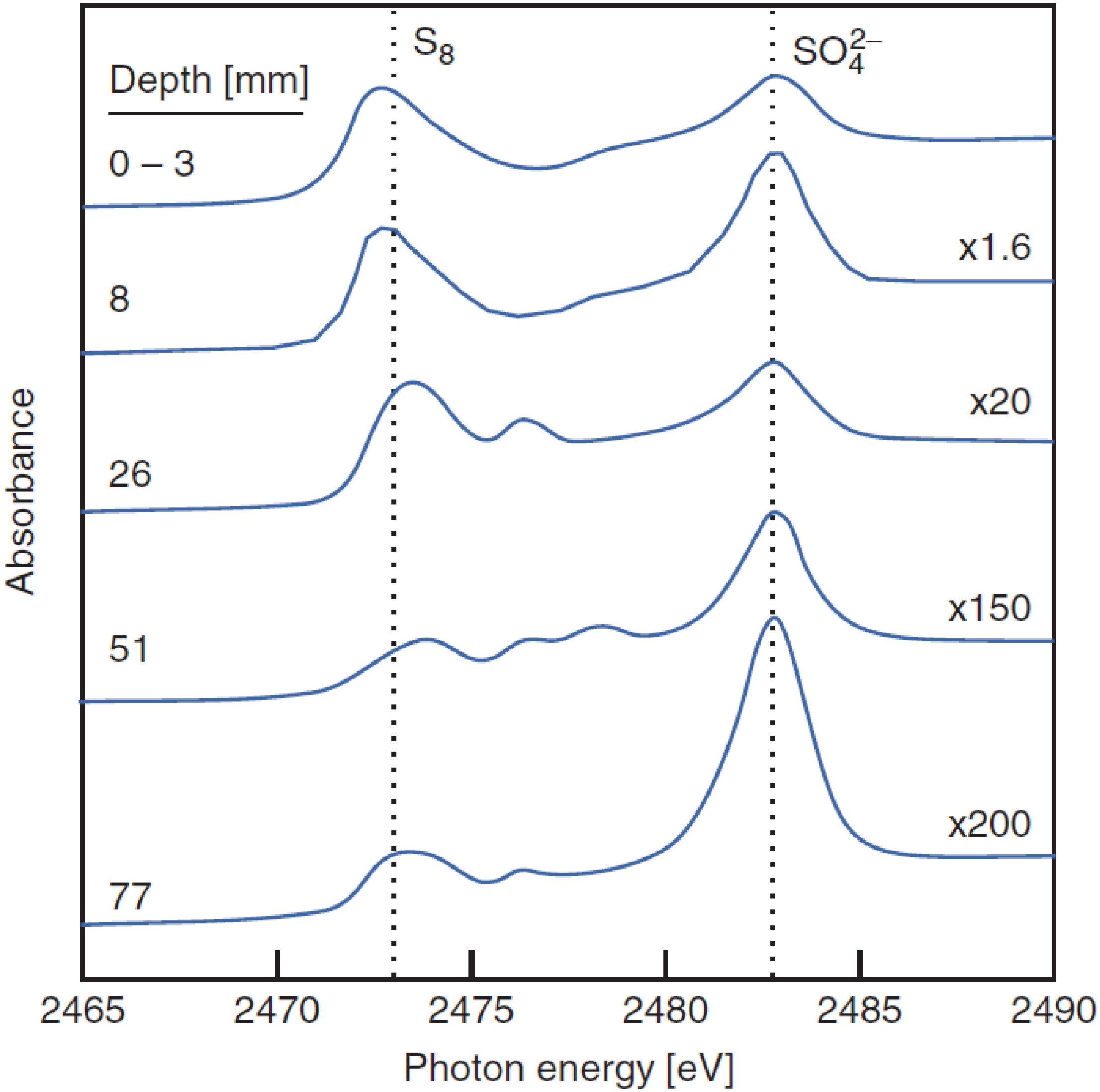

giuliana.aquilanti@elettra.eu

XANES analysis of Fe valence in iron gall inks

- Iron gall inks is one of the most important inks in the history of the western civilization, of a widespread use from the middle ages until the 20th century
- These inks induce degradation of paper
- The two main reasons for iron gall ink corrosion are:
  - Acid hydrolysis
  - Oxidation (catalyzed by ferrous ions)
- Determination of the concentration of Fe^{2+} in inks in historic documents is therefore relevant in assessing the potential risk of further oxidation of cellulose and in devising an effective stabilization treatment

I. Arcon et al., *X-ray Spectrometry*, 36, pp. 199–205, 2007.

giuliana.aquilanti@elettra.eu

XANES analysis of Fe valence in iron gall inks

OR-1

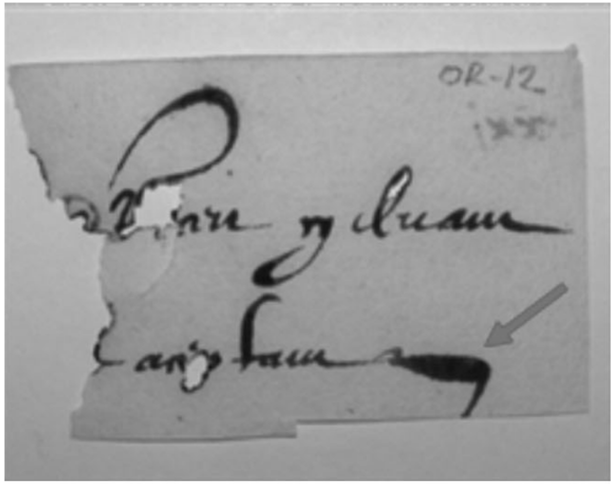

OR-2

OR-4

OR-3

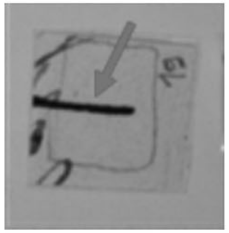

OR-5

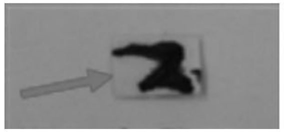

OR-6

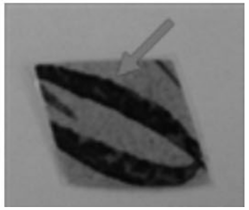

- XANES has been used to determine Fe^{2+}/Fe^{3+}
- Model compounds of iron gall ink have been prepared with different amount of Fe^{2+}/Fe^{3+}
- Standard compounds with well established Fe valence and local symmetry were also measured

I. Arcon et al., *X-ray Spectrometry*, 36, pp. 199–205, 2007.

XANES analysis of Fe valence in iron gall inks

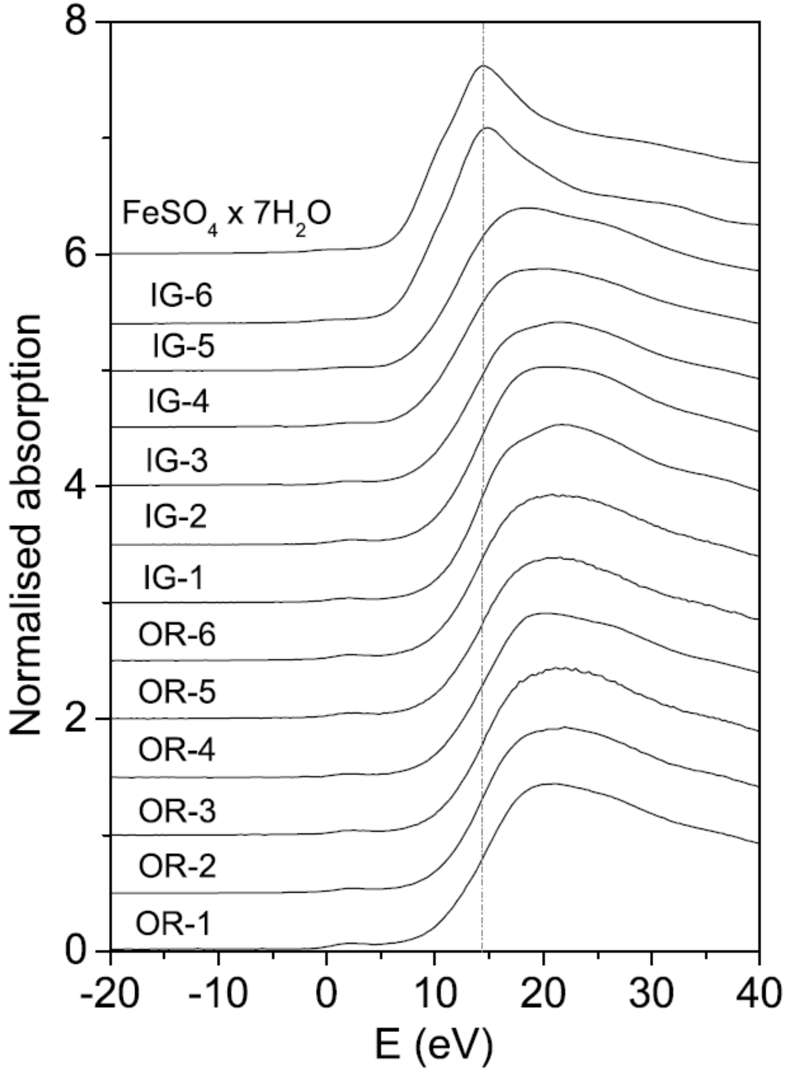

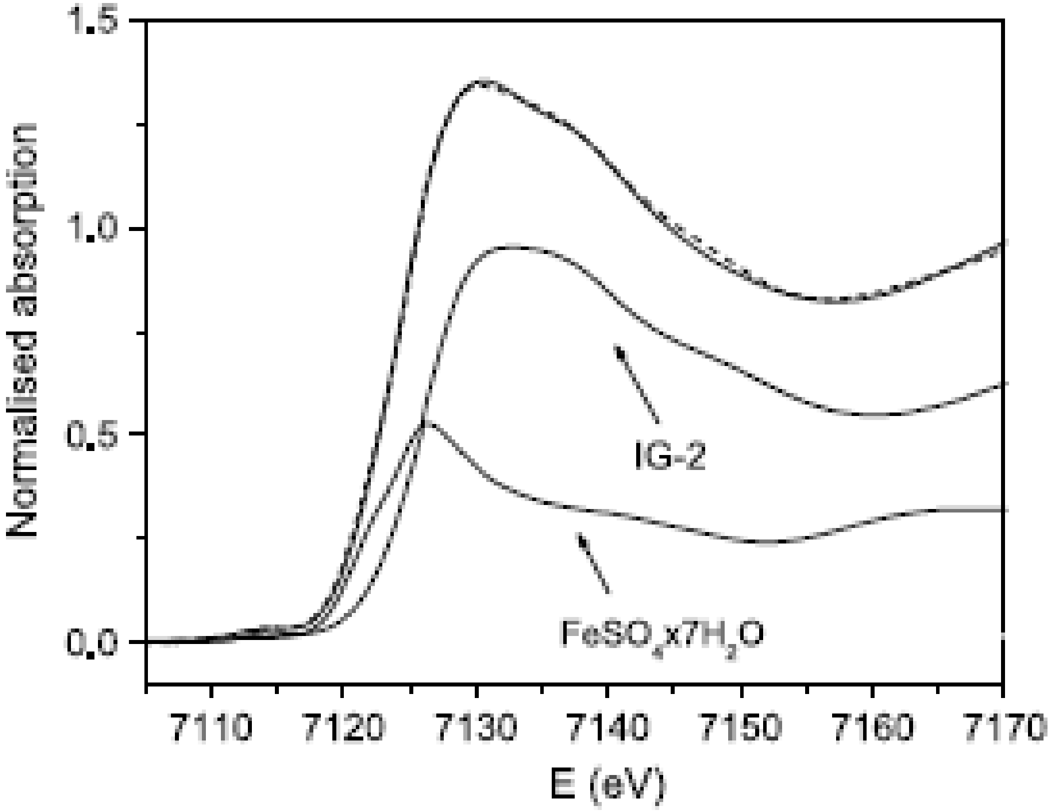

I. Arcon et al., *X-ray Spectrometry*, 36, pp. 199–205, 2007.

Outline

- X-ray absorption
- X-ray absorption fine structure
- XANES
- Some examples of EXAFS and XANES studies for cultural heritage
- EXAFS data analysis

Data treatment: strategy

Step for reducing measured data to μ(E) and then to χ(k):

1. convert measured intensities to μ(E)
2. subtract a smooth pre-edge function, to get rid of any instrumental background, and absorption from other edges.
3. normalize μ(E) to go from 0 to 1, so that it represents 1 absorption event
4. remove a smooth post-edge background function to approximate $\mu_0(E)$ to isolate the XAFS χ.
5. identify the threshold energy E_0, and convert from E to k space: $k = \frac{\sqrt{2m(E - E_0)}}{2}$
6. weight the XAFS χ(k) and Fourier transform from k to R space.
7. isolate the χ(k) for an individual "shell" by Fourier filtering.

Converting raw data to μ(E)

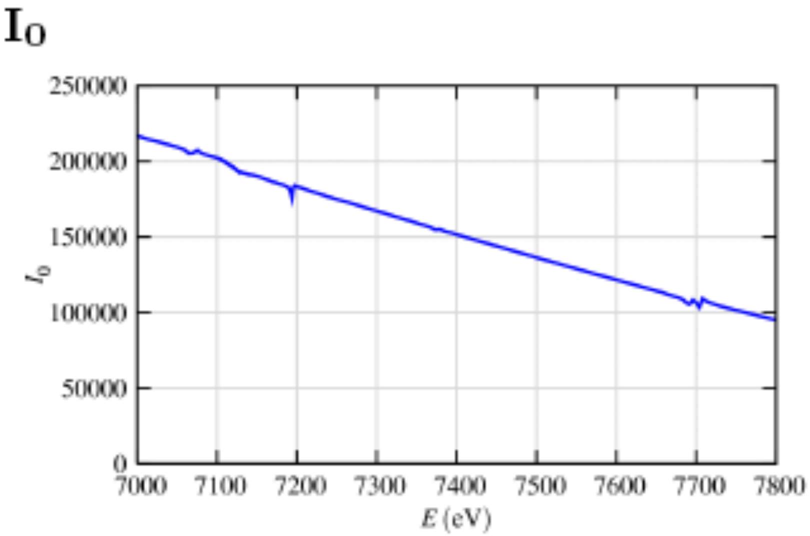

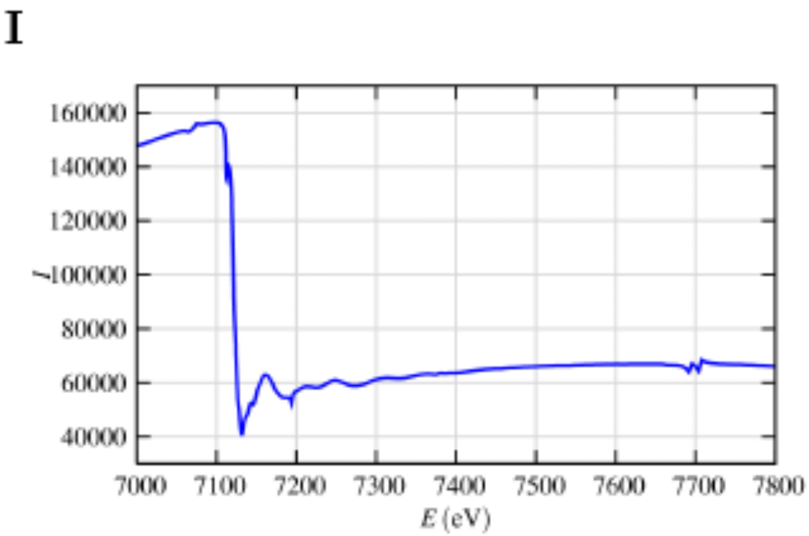

For transmission XAFS:

$$I \ = \ I_0 \exp[-\mu(E)\, t]$$

$$\mu(E)\, t \ = \ \ln\, [I_0/I]$$

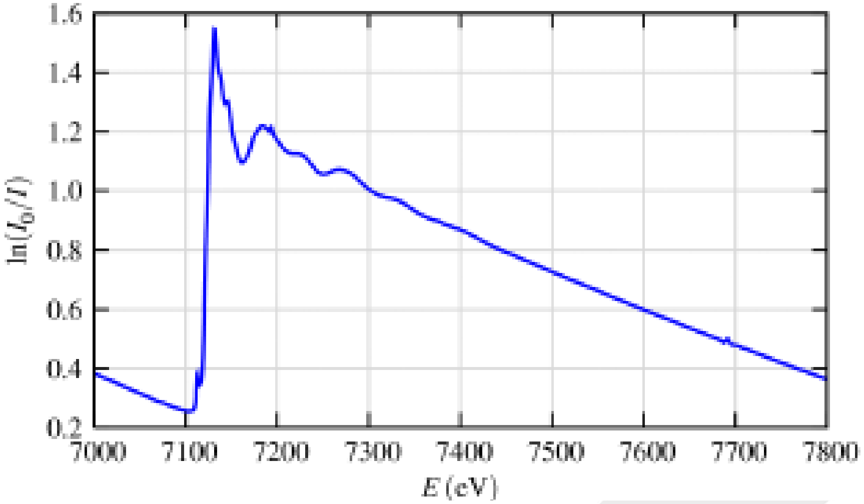

Absorption measurements in real life

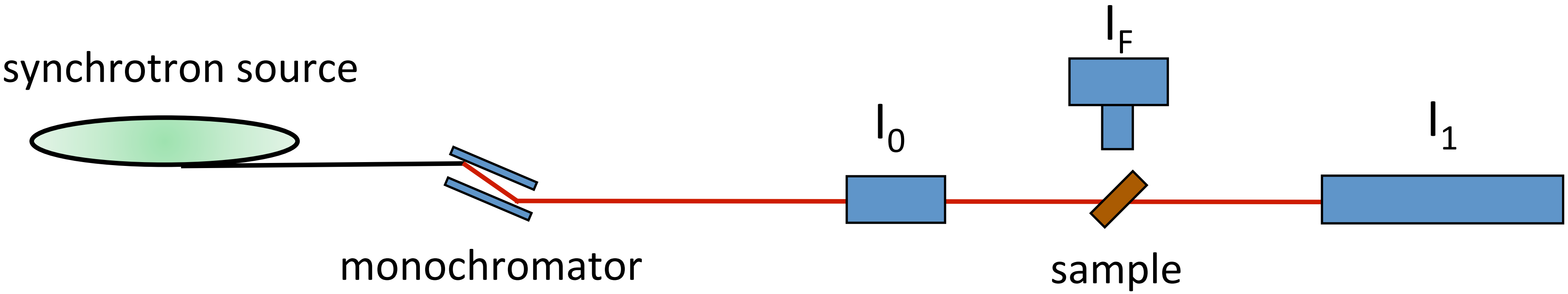

Transmission

The absorption is measured directly by measuring what is transmitted through the sample

Fluorescence

The re-filling the deep core hole is detected. Typically the fluorescent X-ray is measured

Pre-edge subtraction and normalization

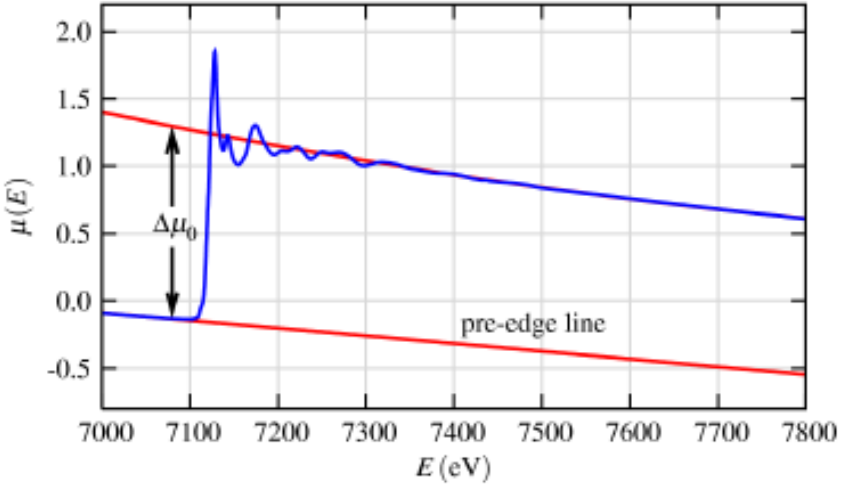

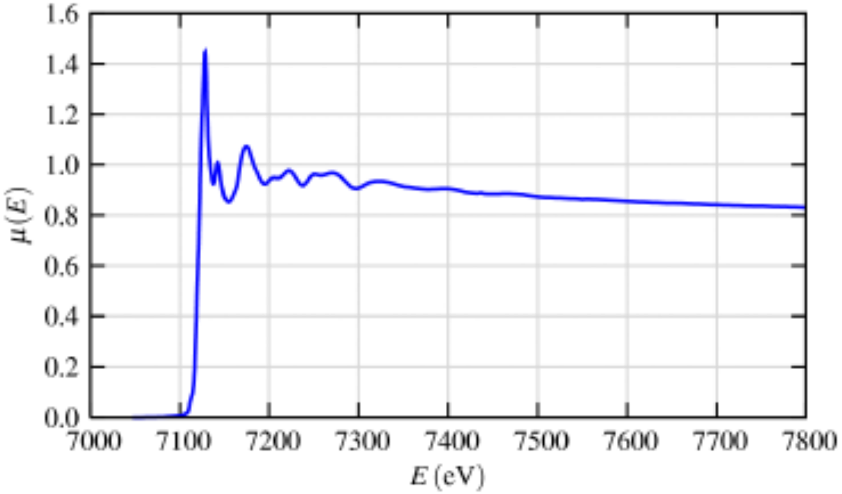

Pre-edge subtraction

We subtract away the background that fits the *pre edge* region. This gets rid of the absorption due to other edges (say, the Fe L_{III} edge).

Normalization

We estimate the *edge step*, $\mu_0(E_0)$ by extrapolating a simple fit to the above μ(E) to the edge.

giuliana.aquilanti@elettra.eu

Determination of E_0

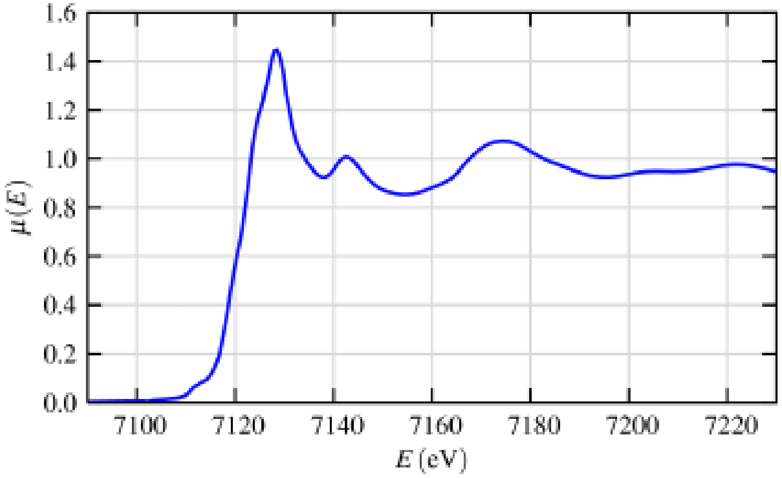

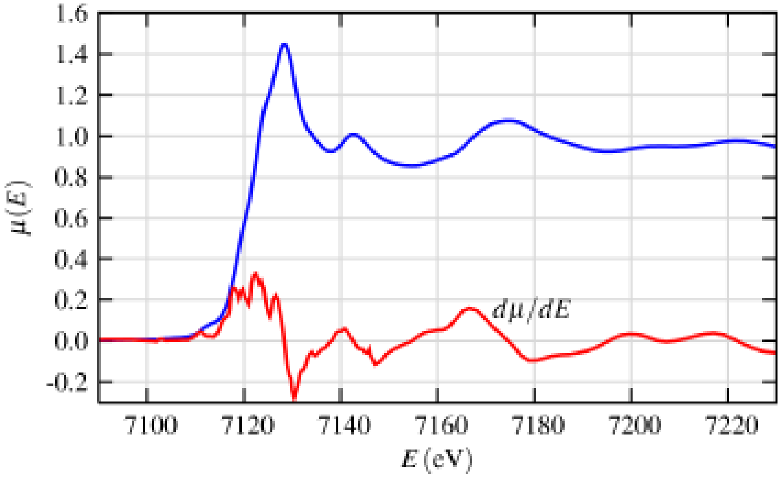

Derivative and E_0

We can select E_0 roughly as the energy with the maximum derivative. This is somewhat arbitrary, so we will keep in mind that we may need to refine this value later on.

giuliana.aquilanti@elettra.eu

Post-edge background subtraction

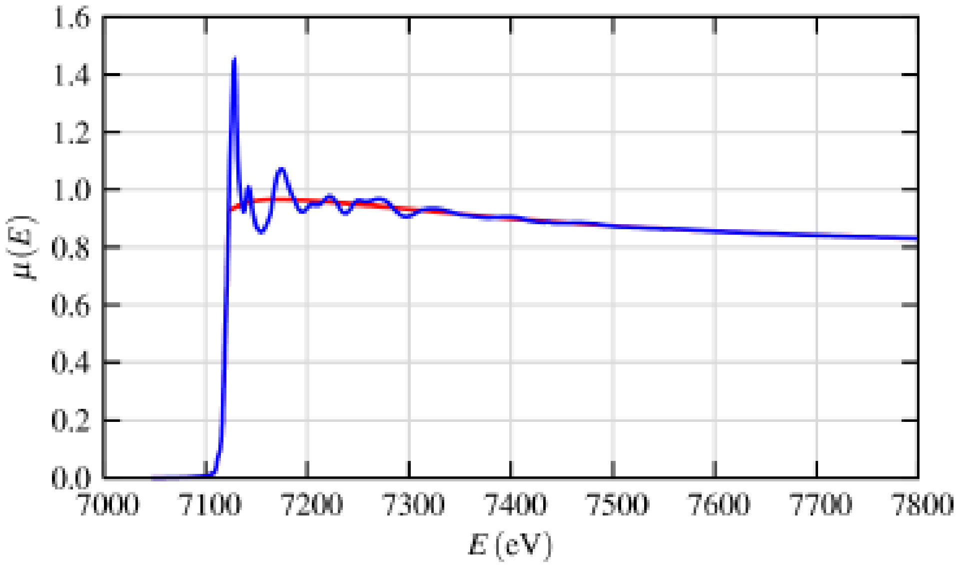

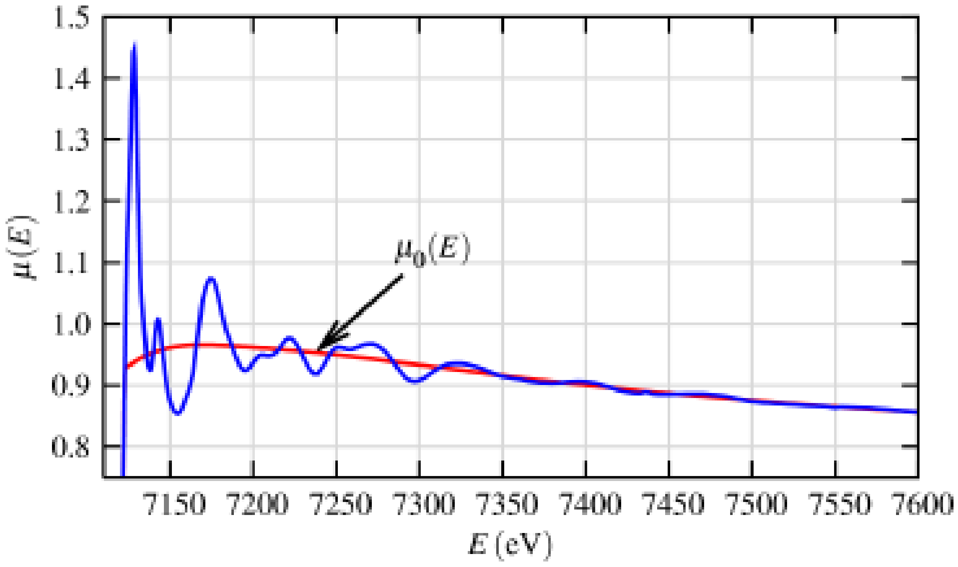

Post-edge background

- We do not have a measurement of $\mu_0(E)$ (the absorption coefficient without neighboring atoms).
- We approximate $\mu_0(E)$ by an adjustable, smooth function: a *spline*.
- A flexible enough spline should not match the $\mu(E)$ and remove all the EXAFS. We want a spline that will match the *low frequency* components of $\mu_0(E)$.

X(k), k-weighting

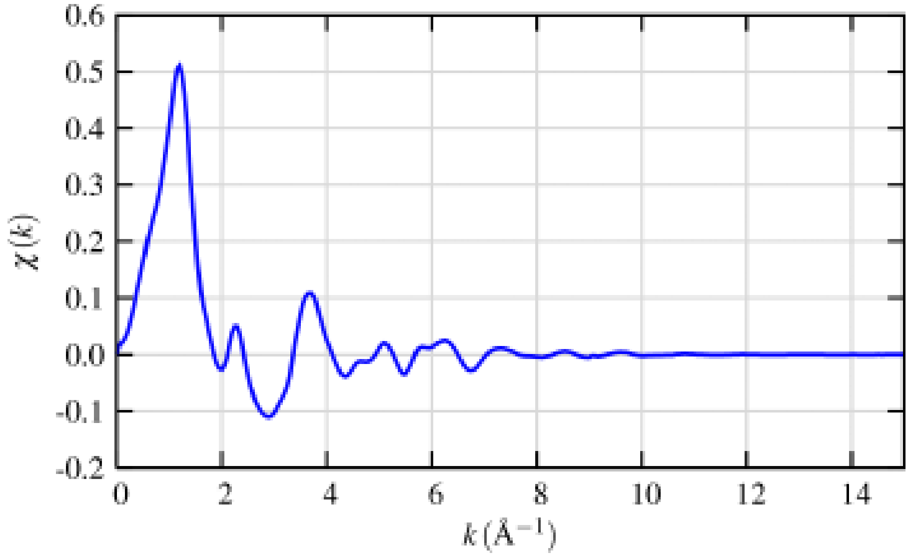

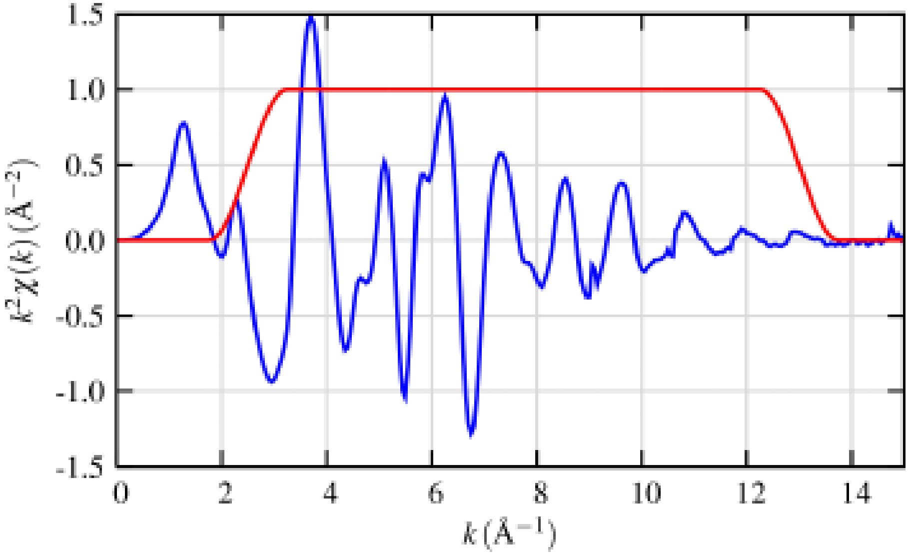

χ(k)

The raw EXAFS χ(k) usually decays quickly with k, and difficult to assess or interpret by itself.
It is customary to weight the higher k portion of the spectra by multiplying by k^2 or k^3.

k-weighted χ(k): $k^2\chi(k)$

χ(k) is composed of sine waves, so we'll Fourier Transform from k to R-space.
To avoid "ringing", we'll multiply by a *window function*.

Fourier Transform: χ(R)

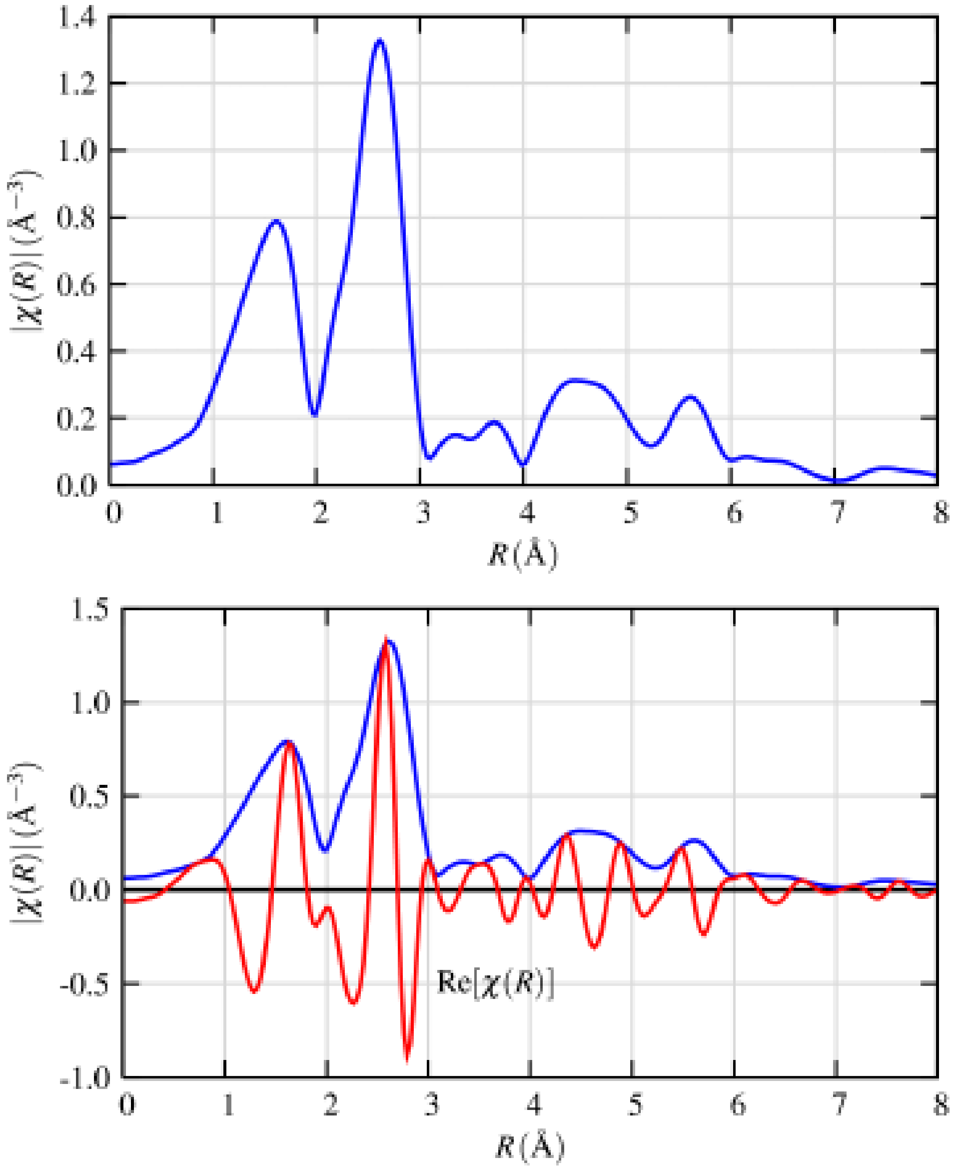

χ(R)

The Fourier Transform of k^2(k) has 2 main peaks, for the first 2 coordination shells: Fe-O and Fe- Fe. The Fe-O distance in FeO is 2.14Å , but the first peak is at 1.66Å . This shift in the first peak is due to the *phase-shift*, δ(k): sin[2kR + δ(k)] .

A shift of -0.5 Å is typical.

χ(R) is complex:

The FT makes c(R) complex. Usually only the amplitude is shown, but there are really oscillations in c(R). Both real and imaginary components are used in modeling.

giuliana.aquilanti@elettra.eu

Fourier filtering

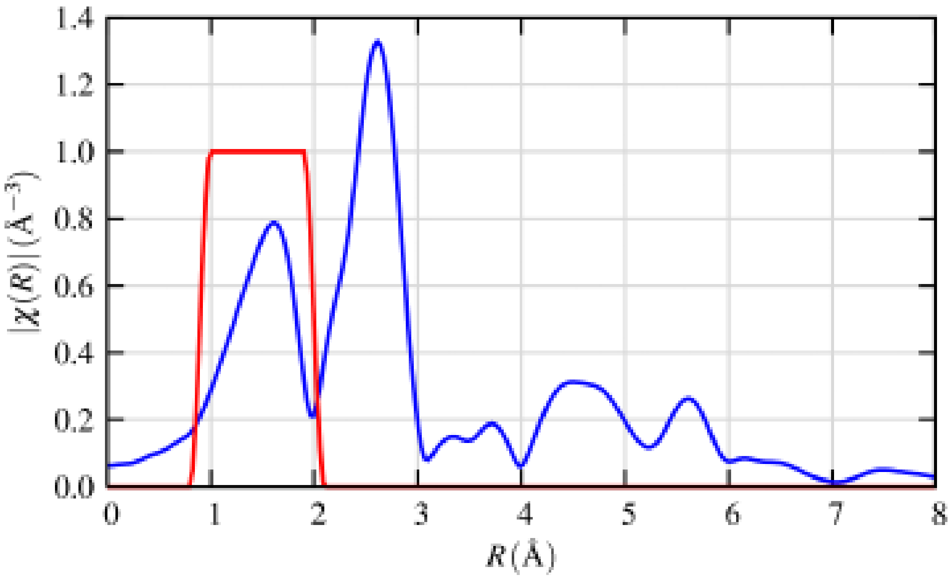

$\chi(R)$ often has well separated peaks for different "shells".

This shell can be isolated by a Filtered Back-Fourier Transform, using the window shown for the first shell of FeO.

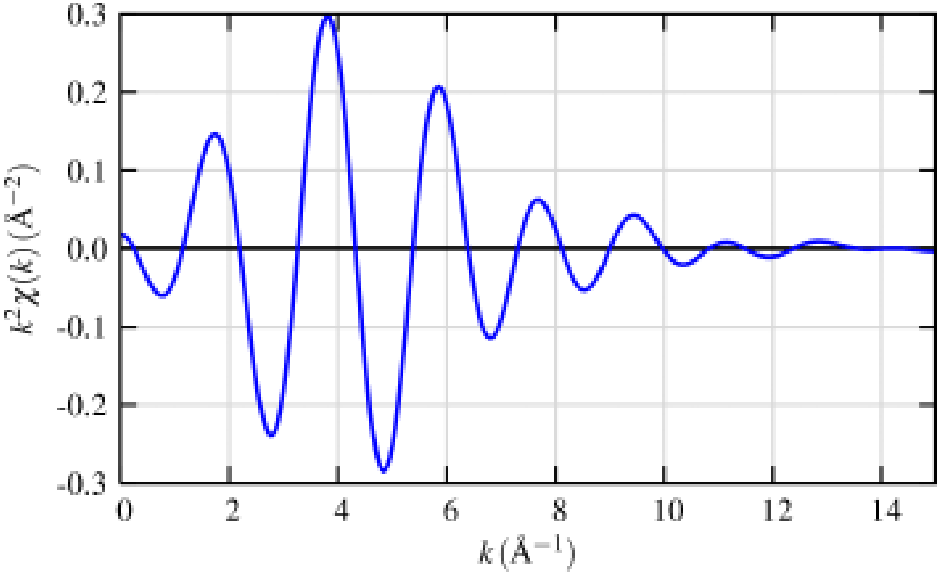

This results in the filtered $\chi(k)$ for the selected shell. Many analysis programs use such filtering to remove shells at higher R.

Beyond the first shell, isolating a shell in this way can be difficult.

giuliana.aquilanti@elettra.eu

The information content of EXAFS

- The number of parameters we can reliably measure from our data is limited:

$$N \approx \frac{2\,\Delta k\,\Delta R}{\pi}$$

  where Δk and ΔR are the k- and R-ranges of the usable data.
- For the typical ranges like k = [3.0, 12.0] $Å^{-1}$ and R = [1.0, 3.0] Å, there are ~ 11 parameters that can be determined from EXAFS.
- The "Goodness of Fit" statistics, and confidence in the measured parameters need to reflect this limited amount of data.
- It is often important to constrain parameters R, N, σ^2 for different paths or even different data sets (different edge elements, temperatures, etc)
- Chemical Plausibility can also be incorporated, either to weed out obviously bad results or to use other knowledge of local coordination, such as the Bond Valence Model (relating valence, distance, and coordination number).
- Use as much other information about the system as possible!

giuliana.aquilanti@elettra.eu

Modeling the first shell of FeO - 1

FeO has a rock-salt structure.

To model the FeO EXAFS, we calculate the scattering amplitude $f(k)$ and phase-shift $\delta(k)$, based on a guess of the structure, with Fe-O distance R = 2.14 Å (a regular octahedral coordination). We will use these functions to *refine* the values R, N, σ^2, and E_0 so our model EXAFS function matches our data.

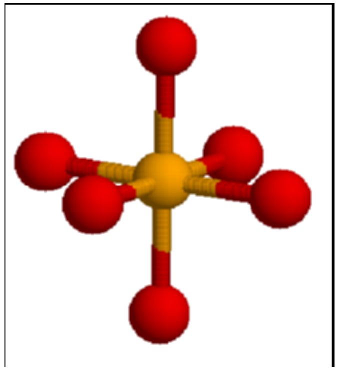

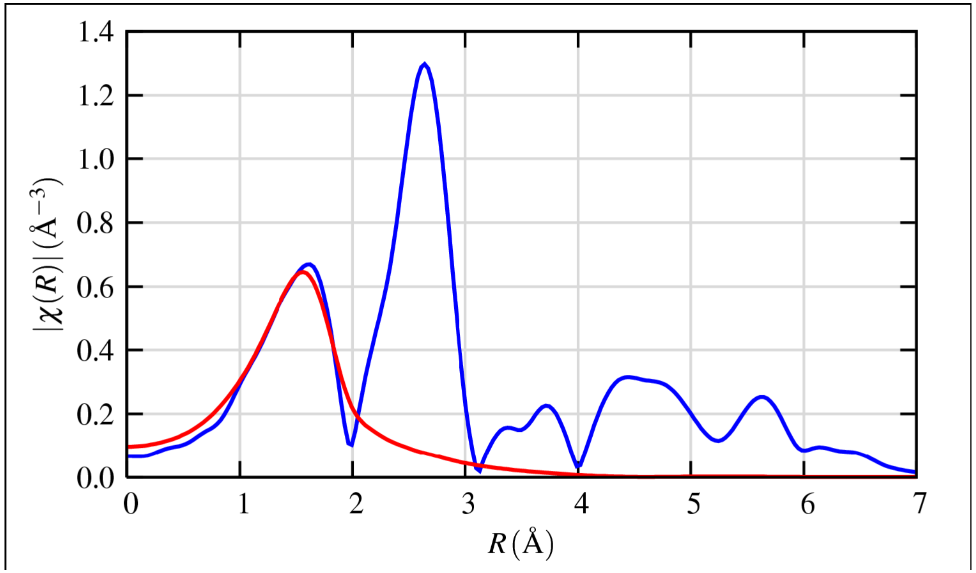

|χ(R)| for FeO (blue), and a 1st shell fit (red).

Fit results

$N = 5.8 \pm 1.8$

$R = 2.10 \pm 0.02$ Å

$E_0 = -3.1 \pm 2.5$ eV

$\sigma^2 = 0.015 \pm 0.005$ Å ^{2}.

giuliana.aquilanti@elettra.eu

Modeling the first shell of FeO - 2

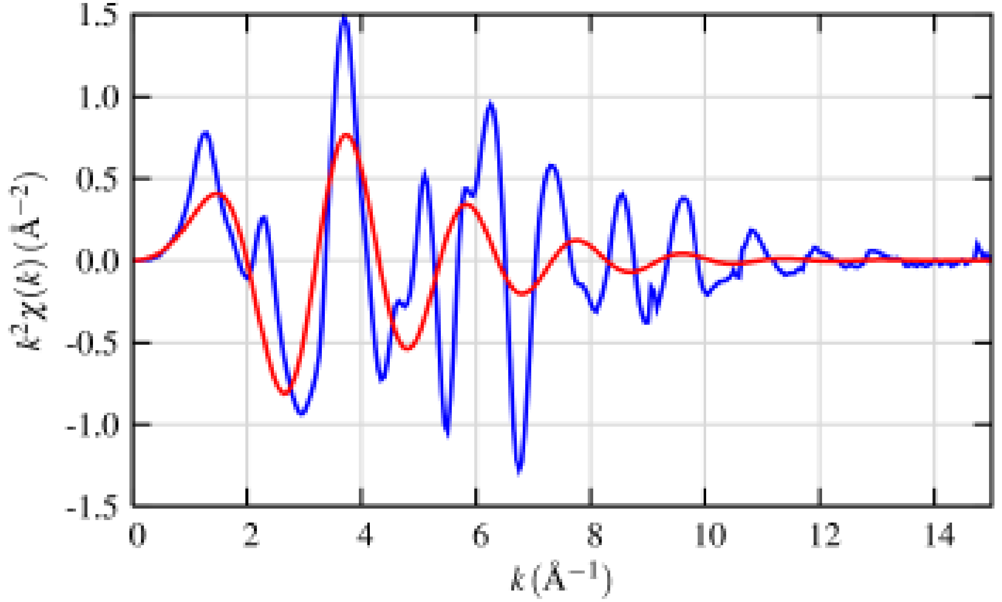

1st shell fit in k space

The 1st shell fit to FeO in k space. There is clearly another component in the XAFS

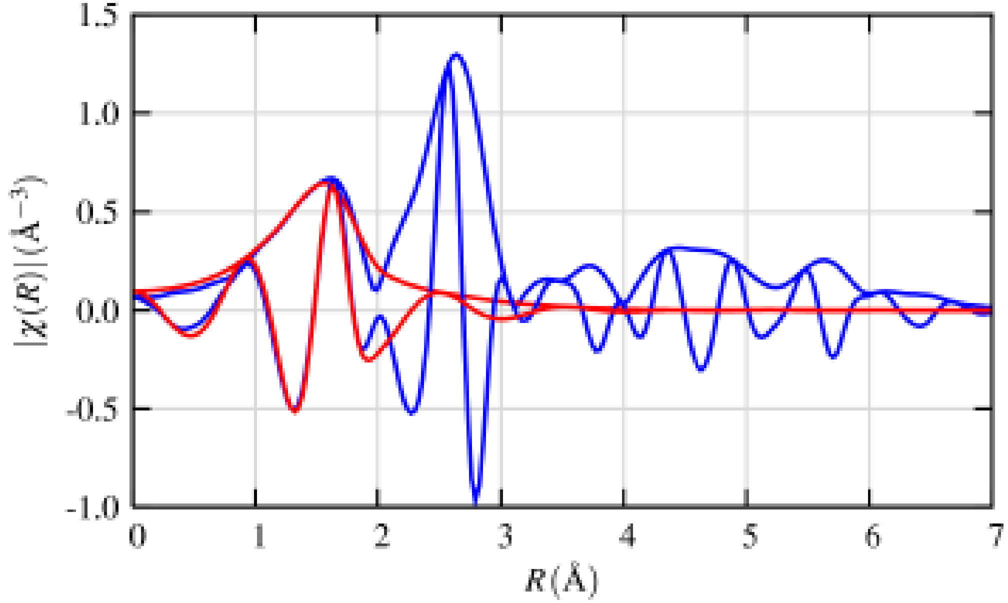

1st shell fit in R space

$|\chi(R)|$ and Re[$\chi(R)$] for FeO (blue), and a 1st shell fit (red).

giuliana.aquilanti@elettra.eu

Modeling the second shell of FeO - 1

To add the second shell Fe to the model, we use calculation for f(k) and δ(k) based on a guess of the Fe-Fe distance, and refine the values R,N, σ^2.

Such a fit gives a result like this:

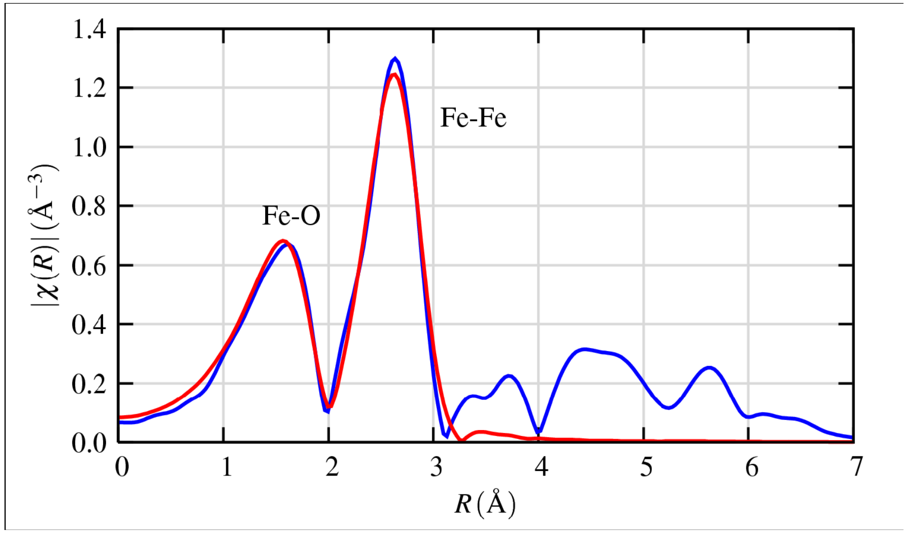

|χ(R)| data for FeO (blue), and fit of 1st and 2nd shells (red).

The results are fairly consistent with the known values for crystalline FeO:

6 O at 2.13Å, 12 Fe at 3.02Å .

Fit results (uncertainties in parentheses):

Shell	N	R (Å)	σ^2 (Å^2)	ΔE_0 (eV)
Fe-O	6.0(1.0)	2.10(.02)	0.015(.003)	-2.1(0.8)
Fe-Fe	11.7(1.3)	3.05(.02)	0.014(.002)	-2.1(0.8)

Modeling the second shell of FeO - 2

Other views of the data and two-shell fit:

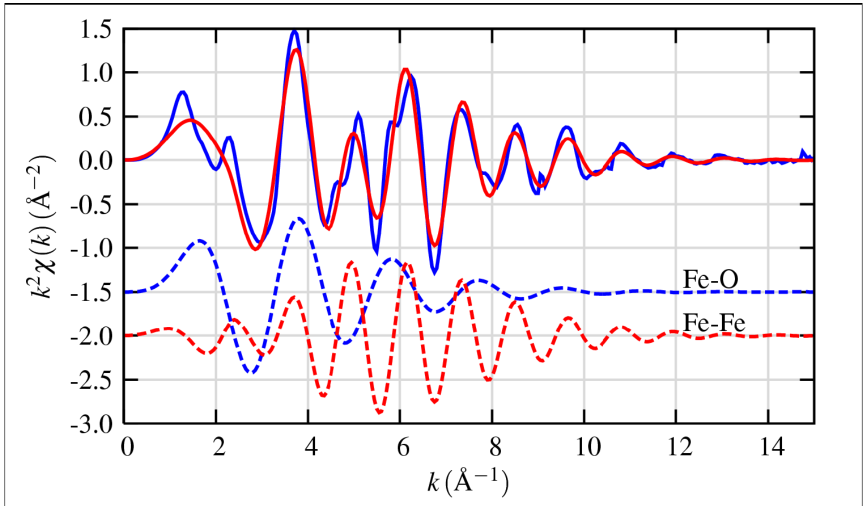

The Fe-Fe EXAFS extends to higher-k than the Fe-O EXAFS.

Even in this simple system, there is some *overlap* of shells in R-space.

The agreement in Re[χ(R)] look especially good – this is how the fits are done.

The modeling can get more complicated than this